Available online at www.sciencedirect.com

ScienceDirect

J. Differential Equations 244 (2008) 1255–1286

Journal of Differential Equations

www.elsevier.com/locate/jde

Connectivity and design of planar global attractors of Sturm type. II: Connection graphs

Bernold Fiedler [a,*], Carlos Rocha [b]

[a] *Institut für Mathematik, Freie Universität Berlin, Arnimallee 2-6, D-14195 Berlin, Germany*
[b] *Instituto Superior Técnico, Avenida Rovisco Pais, 1049-001 Lisboa, Portugal*

Received 5 May 2007; revised 14 September 2007

Available online 26 November 2007

Abstract

Based on a Morse–Smale structure we study planar global attractors $\mathcal{A}_f$ of the scalar reaction–advection–diffusion equation $u_t = u_{xx} + f(x, u, u_x)$ in one space dimension. We assume Neumann boundary conditions on the unit interval, dissipativeness of f, and hyperbolicity of equilibria. We call $\mathcal{A}_f$ Sturm attractor because our results strongly rely on nonlinear nodal properties of Sturm type.

The planar Sturm attractor consists of equilibria of Morse index 0, 1, or 2, and their heteroclinic connecting orbits. The unique heteroclinic orbits between adjacent Morse levels define a plane graph $\mathcal{C}_f$ which we call the connection graph. Its 1-skeleton $\mathcal{C}_f^1$ consists of the unstable manifolds (separatrices) of the index-1 Morse saddles.

We present two results which completely characterize the connection graphs $\mathcal{C}_f$ and their 1-skeletons $\mathcal{C}_f^1$ in purely graph theoretical terms. Connection graphs are characterized by the existence of pairs of Hamiltonian paths with certain chiral restrictions on face passages. Their 1-skeletons are characterized by the existence of cycle-free orientations with certain restrictions on their criticality. Such orientations are called *bipolar* in [H. de Fraysseix, P.O. de Mendez, P. Rosenstiehl, Bipolar orientations revisited, Discrete Appl. Math. 56 (1995) 157–179].

In [B. Fiedler, C. Rocha, Connectivity and design of planar global attractors of Sturm type. I: Orientations and Hamiltonian paths, Crelle J. Reine Angew. Math. (2007), in press] we have shown the equivalence of the two characterizations. Moreover we have established that connection graphs of Sturm attractors indeed satisfy the required properties. In the present paper we show, conversely, how to design a planar Sturm attractor with prescribed plane connection graph or 1-skeleton of the required properties. In [B. Fiedler, C. Rocha, Connectivity and design of planar global attractors of Sturm type. III: Small and Platonic exam-

* Corresponding author.
E-mail addresses: fiedler@math.fu-berlin.de (B. Fiedler), crocha@math.ist.utl.pt (C. Rocha).
URLs: http://dynamics.mi.fu-berlin.de (B. Fiedler), http://www.math.ist.utl.pt/cam/ (C. Rocha).

0022-0396/$ – see front matter
doi:10.1016/j.jde.2007.09.015

ples, 2007, submitted for publication] we describe all planar Sturm attractors with up to 11 equilibria. We also design planar Sturm attractors with prescribed Platonic 1-skeletons.

1. Introduction

Based on a Morse–Smale structure we continue our study [23] of the global spatio-temporal dynamics of the following scalar reaction–advection–diffusion equation in one space dimension

$$u_t = u_{xx} + f(x, u, u_x). \tag{1.1}$$

Here $t \geqslant 0$ denotes time, $0 < x < 1$ denotes space, and we seek solutions $u = u(t, x) \in \mathbb{R}$. To be completely specific we also fix Neumann boundary conditions

$$u_x = 0 \quad \text{at } x = 0 \text{ and } x = 1. \tag{1.2}$$

Our results will hold analogously, though, for other separated boundary conditions; see [3,17,19, 25,38,39].

For nonlinearities $f = f(x, u, p)$ of class C^2 standard theory provides a local solution semigroup $u(t, \cdot) = \mathcal{T}(t)u_0$, $t \geqslant 0$, on initial conditions $u_0 \in X$. For the underlying Banach space X we choose the Sobolev space H^2 intersected with the Neumann condition (1.2). See for example [33,41,47] for a general background.

Our main object is the *global attractor* $\mathcal{A} = \mathcal{A}_f$ of the semigroup $\mathcal{T} = \mathcal{T}_f$. We assume

$$f \in C^2 \quad \text{is dissipative.} \tag{1.3}$$

Here *dissipativeness* requires that there exists a fixed large ball in X in which any solution $u(t, \cdot) = \mathcal{T}(t)u_0$ stays eventually, for all $t \geqslant t(u_0)$. In particular solutions exist globally for all $t \geqslant 0$. For broad surveys on the theory of global attractors we refer to [5,12,15,30,31,35,42,45, 48] and the many references there. We call the specific attractors arising from our setting (1.1), (1.2) *Sturm attractors*.

A Lyapunov function $\mathcal{V}$ of the form

$$\mathcal{V}(u) = \int_0^1 a(x, u, u_x)\, dx \tag{1.4}$$

which is strictly decreasing along all solutions $u(t, \cdot) = \mathcal{T}(t)u_0$, except at equilibria, induces a *gradient-like structure* of the semigroup $\mathcal{T}(t)$; see [36,38,52]. For nonlinearities $f = f(x, u)$ which do not contain advection terms u_x a well-known explicit form of a is $a(x, u, p) = \frac{1}{2}p^2 - F(x, u)$ with primitive $F_u := f$.

To exclude degenerate cases we assume *hyperbolicity* of all equilibria

$$0 = v_{xx} + f(x, v, v_x) \tag{1.5}$$

of (1.1) with Neumann boundary conditions $v_x = 0$ given by (1.2). As usual hyperbolicity of v means that the linearized Sturm–Liouville eigenvalue problem

$$\lambda u = u_{xx} + f_p\big(x, v(x), v_x(x)\big)u_x + f_u\big(x, v(x), v_x(x)\big)u, \tag{1.6}$$

again with Neumann boundary (1.2), possesses only the trivial solution $u \equiv 0$ for $\lambda = 0$. We call the number of positive eigenvalues λ the *unstable dimension* or *Morse index* $i = i(v)$ of the equilibrium v. We number eigenvalues $\lambda = \lambda_k$ such that

$$\lambda_0 > \cdots > \lambda_{i-1} > 0 > \lambda_i > \lambda_{i+1} > \cdots. \tag{1.7}$$

Let $\mathcal{E} = \{v_1, \ldots, v_N\}$ denote the set of all equilibria. Note that $\mathcal{E}$ is finite by dissipativeness of f and hyperbolicity of equilibria. Morse inequalities, Leray–Schauder degree, or a shooting argument in fact show that N is odd. Hyperbolic equilibria v come equipped with local *unstable* and *stable manifolds* $W^u(v)$ and $W^s(v)$ of dimension and codimension $i(v)$, respectively.

As a consequence of the Lyapunov functional (1.4) the global attractor $\mathcal{A}$ of (1.1), (1.2) consists entirely of equilibria and *heteroclinic orbits* $u(t, \cdot)$, which converge to different equilibria for $t \to \pm\infty$. See for example the survey [42] and [18]. In other words Sturm attractors $\mathcal{A}$ consist of just all unstable manifolds

$$\mathcal{A} = \bigcup_{v \in \mathcal{E}} W^u(v). \tag{1.8}$$

The ω-limit set of any trajectory in $W^u(v) \setminus \{v\}$ must in fact consist of a single equilibrium different from v itself due to the gradient-like structure and hyperbolicity. Therefore all non-equilibrium trajectories in $\mathcal{A}$ are heteroclinic.

The *Morse–Smale property* requires transverse intersections of all stable and unstable manifolds of equilibria in addition to hyperbolicity and the gradient-like structure. It was a celebrated result of Angenent and Henry, independently, that this Morse–Smale transversality is, not an additional requirement but, a consequence of hyperbolicity of equilibria; see [1,34]. Surprisingly this fact is based on a generalization of the *Sturm nodal property* first observed by [46] and very successfully revived by [37]. Let $z(u) \leqslant \infty$ denote the number of strict sign changes of $u \in X \setminus \{0\}$. Let $u^1(t, \cdot)$, $u^2(t, \cdot)$ denote any two nonidentical solutions of (1.1), (1.2). Then

$$t \mapsto z\big(u^1(t, \cdot) - u^2(t, \cdot)\big) \tag{1.9}$$

is finite, for any $t > 0$, nonincreasing with t, and drops strictly whenever multiple zeros $u^1 = u^2$, $u^1_x = u^2_x$ occur at any t_0, x_0. See [2]. See [16,20–22,26,29,42] for aspects of nonlinear Sturm theory. It is for this property, central to the entire analysis in the present paper, that we use the term Sturm attractor for the global attractors of (1.1), (1.2).

Our description of Sturm attractors will be based on the *connection graph* $\mathcal{C}_f$ of the global attractor $\mathcal{A}_f$. Vertices of $\mathcal{C}_f$ are the N equilibria $v_1, \ldots, v_N \in \mathcal{E}_f$ of $\mathcal{A}_f$. An edge of $\mathcal{C}_f$ between v_j, v_k indicates the existence of a heteroclinic orbit between equilibria v_j, v_k of adjacent Morse index $i(v_j) = i(v_k) \pm 1$. By Morse–Smale transversality of stable and unstable manifolds, heteroclinic orbits can only run from higher to strictly lower Morse indices. Therefore the connection graph $\mathcal{C}_f$ comes with a natural flow-defined edge orientation: edges can be oriented from higher to lower Morse index. As an aside we already note here that heteroclinic orbits between adjacent Morse levels turn out to be unique, whenever they exist, in the Sturm setting (1.1), (1.2).

We have restricted attention to adjacent Morse levels for the following two reasons. First, Morse–Smale systems possess a *transitivity property* of heteroclinic connections. Let $v_1 \rightsquigarrow v_2$ indicate that there exists a heteroclinic orbit from v_1 to v_2. Then $v_1 \rightsquigarrow v_2$ and $v_2 \rightsquigarrow v_3$ implies $v_1 \rightsquigarrow v_3$. The proof is based on the λ-Lemma; see for example [40]. Second and conversely, special to the Sturm setting (1.1), (1.2), suppose $v_k \rightsquigarrow v_0$ with $i(v_k) = i(v_0) + k$. Then there exist further equilibria $v_1, \dots, v_{k-1}$ such that $i(v_j) = i(v_0) + j$ and $v_k \rightsquigarrow v_{k-1} \rightsquigarrow \cdots \rightsquigarrow v_1 \rightsquigarrow v_0$ connects through successively adjacent Morse levels. This *cascading principle* was first observed in [10]; see also [50]. Together transitivity and cascading imply that our graph $\mathcal{C}_f$ of Morse-adjacent heteroclinic connections settles the question of whether or not there exists a heteroclinic connection, for any pair of equilibria.

As a simplified variant of the full connection graph $\mathcal{C}_f$ we have also introduced its undirected 1-*skeleton* $\mathcal{C}_f^1$. Vertices of $\mathcal{C}_f^1$ are the *sink* equilibria only, i.e., the equilibria v with Morse index $i(v) = 0$. Edges of $\mathcal{C}_f^1$ are the unstable manifolds $W^u(v)$ of *saddle* equilibria, i.e., of equilibria v with $i(v) = 1$. More precisely sink vertices v_j, v_k of $\mathcal{C}_f^1$ are connected by an (undirected) edge if, and only if, there exists a saddle equilibrium w such that $w \rightsquigarrow v_j$ and $w \rightsquigarrow v_k$. The 1-skeleton $\mathcal{C}_f^1$ thus ignores *source* equilibria v in $\mathcal{C}_f$, with $i(v) = 2$, together with their emanating heteroclinics to saddle targets.

The present paper continues our description [23] of all *two-dimensional* Sturm attractors $\mathcal{A}$, i.e., of all global attractors $\mathcal{A}_f$ of (1.1), (1.2), for dissipative nonlinearities f such that all equilibria are hyperbolic of Morse index at most two. Planarity of $\mathcal{A}$ is not just local, restricted to each unstable manifold $W^u(v)$, but holds globally. In fact it has been noted by [7,44] that any L^2-orthogonal projection P of any n-dimensional Sturm attractor $\mathcal{A}_f$ onto the span of the first n eigenfunctions of any selfadjoint Sturm–Liouville eigenvalue problem (1.6) is injective. Moreover $\mathcal{A}_f$ becomes a C^1 graph over the span. More specifically the zero number satisfies

$$z(u_1 - u_2) < \dim \mathcal{A}_f = \max_{\mathcal{E}_f} i(v) \tag{1.10}$$

for any two distinct elements u_1 and u_2 of $\mathcal{A}_f$. The weaker property $z(u_1 - u_2) < i(v)$ for any two distinct elements u_1 and u_2 of the same unstable manifold $W^u(v)$ had been established by [1, 8,34]. Because $z \geqslant n$ on the span of the L^2-orthogonal complement of the first n eigenfunctions of any selfadjoint Sturm–Liouville eigenvalue problem, injectivity of the projection P follows from (1.10). Note that the Sturm–Liouville problem need not be related to the nonlinearity f at all. It only matters that $z \geqslant n$ on the L^2-complement, excepting zero.

Planarity of the connection graphs $\mathcal{C}_f$, $\mathcal{C}_f^1$ does not come as a surprise for two-dimensional Sturm attractors $\mathcal{A}_f$. We simply identify the connection graph with the heteroclinic orbits between equilibria of adjacent Morse levels via the planar embedding P.

To formulate our main results on the structure of these connection graphs we therefore collect some terminology concerning plane graphs G next. See also [6], Sections 1.6 and 11.2. We call a graph G *plane*, $G \subseteq \mathbb{R}^2$, if its vertices v_j and edges $e_{jk} = v_j v_k$ are embedded in the plane as points and continuous curves, respectively, such that edges neither intersect nor self-intersect, except possible at their vertex end points v_j, v_k. A *loop* is an edge $v_k v_k$ with identical end points v_k; we only consider graphs without loops below. A *multigraph* is allowed to possess several edges e_{jk}^ℓ connecting the same pair of vertices v_j and v_k. Rather than assigning an integer weight to a single edge we represent multiple edges by multiple nonintersecting curves sharing the same end point vertices. We call any multigraph G *finite* if G consists of finitely many vertices and edges. Any finite plane multigraph G decomposes its complement $\mathbb{R}^2 \setminus G$ into finitely many

connected components called the *regions* or *faces* of G. Exactly one of the regions is unbounded, and its boundary vertices and edges are called the *boundary* ∂G of G. Unless unboundedness is stated explicitly though, by faces we always mean bounded faces below.

A path traverses any sequence $e^{\ell_1}_{k_0k_1}, e^{\ell_2}_{k_1k_2}, \ldots, e^{\ell_r}_{k_{r-1}k_r}$ of distinct multi-edges via distinct vertices. In the exceptional case $k_0 = k_r$ where the first and last vertex only are allowed to coincide, a path is called a *cycle* or *closed*. A (not necessarily closed) path which visits each vertex exactly once is called a *Hamiltonian path*. A *Hamiltonian cycle*, similarly, is a cycle which is a Hamiltonian path.

Directed multigraphs are multigraphs together with an orientation for each edge. Multigraphs can be oriented, i.e., can be assigned an edge orientation. Conversely any directed multigraph can be made undirected simply by forgetting the orientation. Directed paths, directed Hamiltonian paths, and di-cycles (i.e., directed cycles), are required to traverse edges in the given orientation. A vertex $\underline{v}$ of a directed multigraph is called a *directed source* (short: *di-source*) if all its edges point away from it. If all its edges point toward $\bar{v}$ then we call $\bar{v}$ a *di-sink*. We also call $\underline{v}$ a (local) maximum and $\bar{v}$ a (local) minimum. We caution the reader that this notion for vertices in directed multigraphs differs from the Morse notion of source and sink equilibria in planar global attractors $\mathcal{A}_f$ based on their Morse index to be 0 or 2, respectively.

We call a graph G *connected* if any two vertices v_{k_0}, v_{k_r} can be joined by a path of suitable length. For finite connected, plane multigraphs with N vertices, m edges and r bounded faces we recall the Euler characteristic

$$N - m + r = 1. \tag{1.11}$$

We call a plane multigraph *cellular* if each of its (bounded) faces F is bounded by an (undirected) cycle of distinct edges and vertices. See Fig. 1 for illustration. In other words each bounded face F is the interior of a plane (topological) n-gon, for some $n \geqslant 2$. In particular the closure of each bounded face is homeomorphic to a 2-disk.

Each boundary edge $e \subseteq \partial G$ is the boundary of at most one bounded face. Each other edge, called *interior*, is in the boundary of exactly two bounded faces. We note a slight asymmetry in the role of the unbounded face. Under compactification of $\mathbb{R}^2$ to the 2-sphere S^2 the previously unbounded open face will be homeomorphic to an open 2-disk but will not necessarily become a cell of the resulting graph on S^2. The simplest connected example is the graph G of two vertices v_1, v_2 with a single edge joining them.

We are now ready to state the first variant of our main result. We exclude the case of a trivial Sturm attractor $\mathcal{A}_f$ which consist of only one single globally attracting equilibrium.

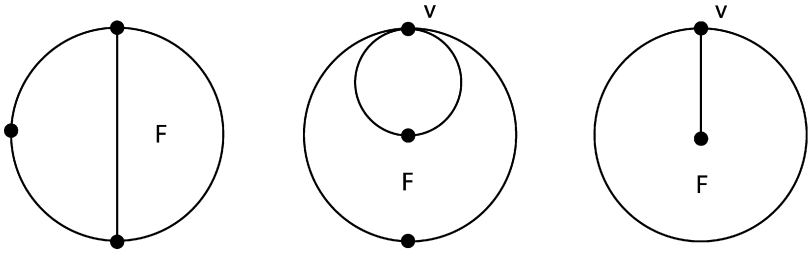

Fig. 1. Cellular and non-cellular multigraphs. Left: cellular. Center: not cellular (doubly traversed vertex v on face boundary F). Right: not cellular (doubly traversed edge on face boundary).

Theorem 1.1. *A graph G is the 1-skeleton $\mathcal{C}_f^1$ of the connection graph $\mathcal{C}_f$ of some at most two-dimensional nontrivial Sturm attractor $\mathcal{A}_f$ with only hyperbolic equilibria if, and only if, G satisfies the following two properties*:

(i) *G is a finite, connected, plane, cellular multigraph without loops, and*
(ii) *G possesses an orientation with exactly one di-sink $\bar{v}$ and one di-source, $\underline{v}$, both on the boundary ∂G, and without di-cycles.*

To say that one plane graph G "is" another plane graph $\tilde{G}$, here and below, indicates an *isomorphism*. The standard notion of graph isomorphism is a vertex bijection which preserves edges. For our plane graphs we require a homeomorphism of the plane graph, including its bounded faces, which maps edge curves to edge curves and vertices to vertices. Combinatorially it is sufficient to preserve face boundaries, in addition to the usual notion.

An orientation of G without di-cycles, as in part (ii) of Theorem 1.1, equivalently defines a partial order on the vertices of G such that the orientation points downhill. In that sense we may call $\bar{v}, \underline{v}$ the unique minimum, maximum of this order, respectively. Such orientations are called *bipolar* with *poles* $\underline{v}, \bar{v}$ in the survey [27], which also reviews several other applications.

We note that the full connection graph $\mathcal{C}_f$ and its flow-oriented variant can both be reconstructed uniquely from their 1-skeleton $\mathcal{C}_f^1$. In fact we detail this construction next for arbitrary finite, plane, cellular multigraphs G without loops. Motivated by $\mathcal{C}_f$ and its 1-skeleton we call the vertices of G *Morse sinks*. Starting from G bisect each edge by an additional vertex. Call the bisecting vertices *Morse saddles*. In each (bounded) face insert one additional vertex and call it a *Morse source*. Draw an edge from each Morse source to the n bisecting Morse saddles on the boundary of its face. We call the resulting undirected graph G_2 the *filled graph* of G. By construction G is the 1-skeleton of its filled graph G_2. Obviously there is a "flow" directed variant of this construction. We just orient bisected edges away from their bisecting Morse saddles, and edges in bounded faces of G away from their Morse sources. Since this filling procedure decomposes each face of the 1-skeleton into quadrilaterals it is sometimes called a *quadrangulation*.

To formulate our characterization of connection graphs $\mathcal{C}_f$, rather than their 1-skeletons $\mathcal{C}_f^1$, we need to recall one last concept from [23]. Consider the filled graph G_2 of any finite, connected, plane, cellular multigraph G without loops. We call a Hamiltonian path h_0 in G_2 a *boundary Z-Hamiltonian path* if the properties (a)–(c) below all hold. Properties (b), (c) restrict the path h_0 as it crosses through any Morse source w in a face F. Let $\dots v_{-2}v_{-1}wv_1v_2\dots$ denote the vertex sequence along h_0. Then $v_{\pm 1}$ are Morse saddles on the face boundary ∂F. The vertices $v_{\pm 2}$ are Morse sinks, or Morse sources other than w and outside F. If v_{-2} or v_{+2} is a Morse sink then it belongs to ∂F. Since ∂F contains at least four vertices, and v_1, v_2 are immediate successors, we can then speak of a clockwise or counter-clockwise direction of the arc v_1v_2 from v_1 to v_2, uniquely, and similarly for $v_{-2}v_{-1}$. Specifically we require

(a) "Boundary":
h_0 starts at some vertex $\underline{v}$ in the boundary ∂G and terminates at another boundary vertex $\bar{v}$.
(b) "No right turn exit":
Whenever $h_0 = \dots wv_1v_2\dots$ exits any Morse source w of a face F then the arc v_1v_2 is not on ∂F in clockwise direction.
(c) "No left turn entry":
Whenever $h_0 = \dots v_{-2}v_{-1}w\dots$ enters any Morse source w of a face F then the arc $v_{-2}v_{-1}$ is not on ∂F in clockwise direction.

The letter Z graphically indicates the admissible behavior in case both the exit arc v_1v_2, on top, and the entry arc $v_{-2}v_{-1}$, on bottom, are on ∂F: right turn entry and left turn exit. Note however that h_0 is also permitted to connect Morse sources of adjacent faces through the bisecting Morse saddle of a shared edge without creating arcs on ∂F at all. Also note that the reverse path $h_0^- = \dots v_2v_1wv_{-1}v_{-2}\dots$ of h_0 is boundary Z-Hamiltonian whenever h_0 is, albeit with reversed roles of the start and termination points $\underline{v}$ and $\bar{v}$.

By plain reflection κ we can also define (*boundary*) *S-Hamiltonian paths* h_1: we simply require the reflected path $h_0 := \kappa h_1$ to be Z-Hamiltonian for the reflected graph κG_2. In other words the S-Hamiltonian path h_1 is neither permitted right turns, upon face entry, nor left turns upon exit. By a (*boundary*) *ZS-Hamiltonian pair* (h_0, h_1) we mean a Z-Hamiltonian path h_0 and

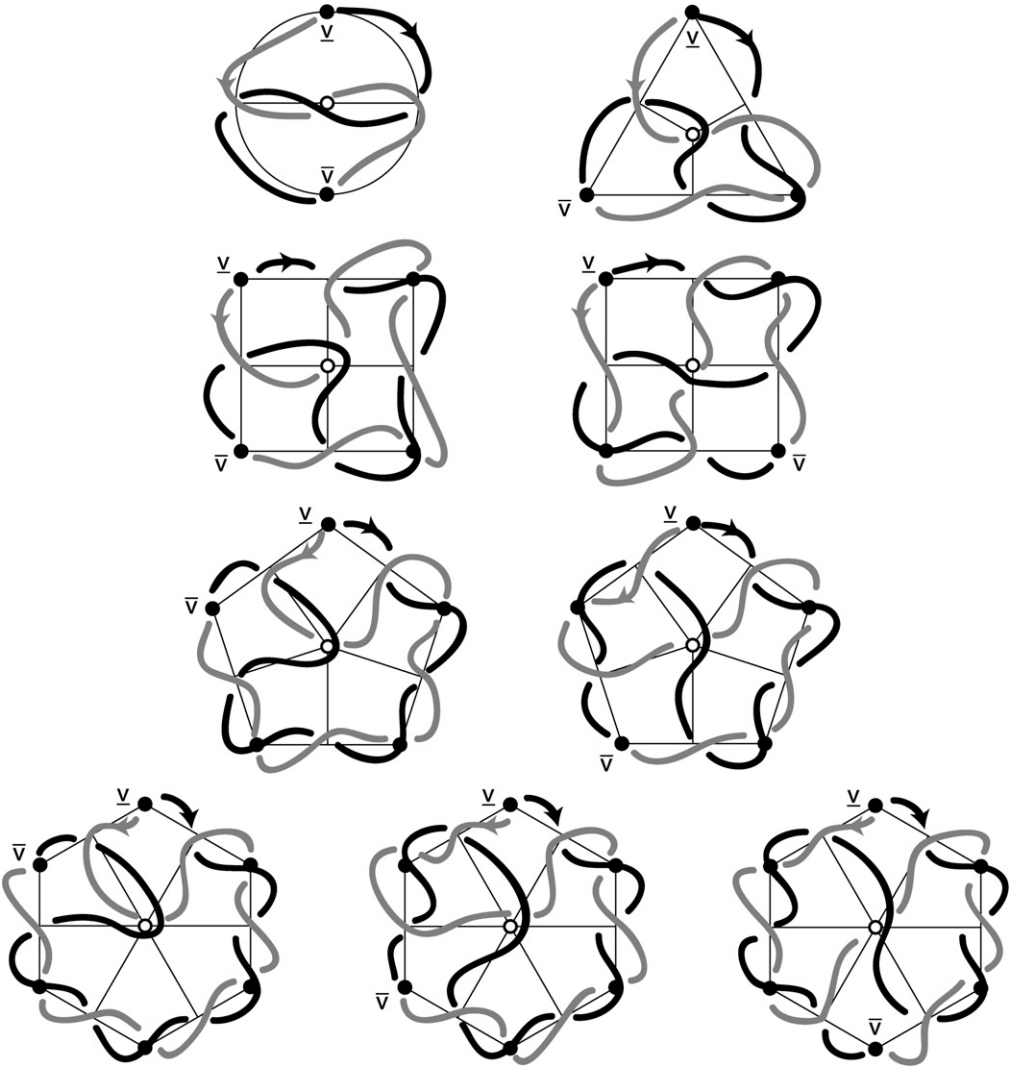

Fig. 2. Boundary Hamiltonian pairs (h_0, h_1) for n-gons, $n = 2, \dots, 6$. Path h_0 black, path h_1 gray.

an S-Hamiltonian path h_1 in G_2, both of which start at the same vertex $\underline{v}$ and terminate at the same distinct vertex $\bar{v}$ in G. See Fig. 2 for 9 examples.

Our concept of ZS-Hamiltonian pairs (h_0, h_1) is motivated, as we have seen in [23], by the fact that the ordering of equilibria v_k of the Sturm PDE (1.1), (1.2), alias vertices of the connection graph $\mathcal{C}_f$, by their boundary values $v_k(x)$ at $x = 0, 1$, respectively, defines a pair of Z- and S-Hamiltonian paths with properties (a)–(c).

Theorem 1.2. *A graph G_2 is the connection graph $\mathcal{C}_f$ of some nontrivial at most two-dimensional Sturm attractor $\mathcal{A}_f$ with only hyperbolic equilibria if, and only if, G_2 satisfies the following two properties*:

(i) *G_2 is the filled graph of a finite, connected, plane, cellular multigraph G without loops, and*
(ii) *G_2 possesses a boundary ZS-Hamiltonian pair (h_0, h_1) which starts and ends at two distinct vertices $\underline{v}$, $\bar{v}$ in the boundary ∂G.*

The "flow" directed filled graph G_2 then coincides with the flow directed connection graph $\mathcal{C}_f$.

In [23] we have already proved the "only if" part of Theorems 1.1 and 1.2. As a main preparation we have proved the equivalence of the bipolar orientations of Theorem 1.1(ii) with the ZS-Hamiltonian pairs of Theorem 1.2(ii). This equivalence is a purely graph theoretic statement on plane graphs and can be formulated as follows.

Theorem 1.3. *Let G be a finite, connected, plane, cellular multigraph without loops. Let the quadrangulation G_2 denote the filled graph of G. Then the following two statements are equivalent.*

(i) *G possesses an orientation G^d with exactly one di-source $\underline{v}$ and one di-sink $\bar{v}$, both on the boundary ∂G, and without directed cycles.*
(ii) *G_2 possesses a boundary ZS-Hamiltonian pair (h_0, h_1) between $\underline{v}$ and $\bar{v}$, in the sense of properties* (a)–(c) *preceding Theorem* 1.2.

The point of the two equivalent formulations later on will be that bipolar orientations of G define unique boundary Z- and S-Hamiltonian paths h_0 and h_1 in G_2, which can then be interpreted as the ordering of equilibria v_k by their boundary values at $x = 0, 1$, respectively. These orders in turn determine the global Sturm attractor $\mathcal{A}_f$. In fact the 1-skeleton $\mathcal{C}_f^1$ and the connection graph $\mathcal{C}_f$ will be shown to coincide with the prescribed 1-skeleton G and its filled counterpart G_2, respectively.

So far we have shown that the 1-skeleton $G = \mathcal{C}_f^1$ of the connection graph $G_2 = \mathcal{C}_f$ of any two-dimensional nontrivial Sturm attractor $\mathcal{A}_f$ with hyperbolic equilibria satisfies properties (i), (ii) of Theorem 1.1. See [23]. Together with Theorem 1.3 this also shows that properties (i), (ii) of Theorem 1.2 hold for the connection graph $G_2 = \mathcal{C}_f$.

It therefore remains to prove that, conversely, any pair G, G_2 with the properties of Theorems 1.1 and 1.2 indeed arises as a 1-skeleton $\mathcal{C}_f^1$ and its connection graph $\mathcal{C}_f$, respectively, for some dissipative nonlinearity f with at most two-dimensional Sturm attractor $\mathcal{A}_f$ and hyperbolic equilibria. In fact we will have to address the converse part of Theorem 1.2 only, again in view of the equivalence in Theorem 1.3. In particular we are given G_2 with a given boundary

ZS-Hamiltonian pair (h_0, h_1) from the di-source $\underline{v}$ to the di-sink $\bar{v}$ of the oriented 1-skeleton G^d of G_2.

To prove the converse part of Theorem 1.2 we first review in Section 2 the precise role of the boundary order of equilibria, alias the boundary *ZS*-Hamiltonian pair (h_0, h_1), for the characterization of Sturm attractors $\mathcal{A}_f$ and their connection graphs $\mathcal{C}_f$. In particular we introduce the Sturm permutations $\pi = h_0^{-1} \circ h_1$ and show how they determine Morse indices of equilibria, the zero number of their differences, and the connection graph. We address the special case of an n-gon connection graph and attractor in Section 3. Section 4 generalizes this paradigm to any general n-gon face within a planar Sturm attractor. In Section 5 we complete the proof of Theorem 1.2. We show how our general construction of boundary *ZS*-Hamiltonian pairs (h_0, h_1) indeed gives rise to nonlinearities f with the prescribed connection graph $\mathcal{C}_f = G_2$. We conclude in Section 6 with a sketch of bifurcations of Sturm attractors and an alternative approach to our results. For illustration purposes we discuss and classify all planar Sturm attractors with up to 11 equilibria in the sequel [24]. We also realize all classical plane Platonic graphs: tetrahedron, cube, octahedron, dodecahedron, and icosahedron.

2. Sturm attractors, Hamiltonian paths and Sturm permutations

In the present section we outline the role that the boundary *ZS*-Hamiltonian pair (h_0, h_1) will play in the connection graph $\mathcal{C}_f$ and the Sturm attractor $\mathcal{A}_f$ in subsequent sections. See also [26,42] for surveys.

The role of h_0, h_1 originates from the ordering of the hyperbolic equilibria

$$\mathcal{E}_f = \{v_1, \dots, v_N\} \subsetneqq \mathcal{A}_f \tag{2.1}$$

on the boundaries $x = 0, 1$, respectively. We define the *boundary permutations* $h_j = h_j^f \in S_N$ by the boundary order

$$v_{h_j(1)}(x) < v_{h_j(2)}(x) < \cdots < v_{h_j(N)}(x) \quad \text{at } x = j = 0, 1. \tag{2.2}$$

The central object in the classification of Sturm attractors, ever since it was first introduced by Fusco and Rocha in [28], is then the *Sturm permutation* $\pi = \pi_f$ defined by

$$\pi := h_0^{-1} \circ h_1. \tag{2.3}$$

Relabeling equilibria by any permutation $\sigma \in S_N$ corresponds to replacing h_j by $\sigma \circ h_j$. This does not affect the Sturm permutation π. For example we may label the equilibria $v_1, \dots, v_N$ such that $h_0 = \mathrm{id}$ is the identity permutation, and thus $v_1 < v_2 < \cdots < v_N$ at $x = 0$. Then $\pi = h_1$ simply keeps track of the order

$$v_{\pi(1)} < v_{\pi(2)} < \cdots < v_{\pi(N)} \quad \text{at } x = 1. \tag{2.4}$$

For simplicity of presentation we fix this labeling in the present section.

The Sturm permutations $\pi = \pi_f$ encode geometric and dynamical information on the Sturm attractors $\mathcal{A} = \mathcal{A}_f$ and, in fact, make the study of their connection graphs $\mathcal{C}_f$ a combinatorial task. We describe some of these results next, as they have been obtained over the past decades, starting with preliminary results in [9–11,14,32,34] for nonlinearities $f = f(u)$.

In [21] it has been observed that any permutation $\pi \in S_N$ is a Sturm permutation, i.e., $\pi = \pi_f$ for some dissipative nonlinearity $f = f(x, u, u_x)$ with only hyperbolic equilibria, if, and only if, π is a *dissipative Morse meander*. We explain these three notions next.

We call a permutation $\pi \in S_N$ *dissipative*, whenever N is odd and $\pi(1) = 1$, $\pi(N) = N$ are fixed under π.

We call a permutation $\pi \in S_N$ *Morse*, whenever the following N quantities i_j are all nonnegative:

$$i_j := \sum_{\iota=1}^{j-1} (-1)^{\iota+1} \operatorname{sign}\bigl(\pi^{-1}(\iota+1) - \pi^{-1}(\iota)\bigr). \tag{2.5}$$

Note $i_1 = 0$ by the empty sum, and $i_N = 0$ for dissipative π.

Following Arnol'd [4], we call $\pi \in S_N$ a *meander* permutation, if the following property holds. Whenever $\pi^{-1}(j')$ is between $\pi^{-1}(j)$ and $\pi^{-1}(j+1)$, and j, j' have the same parity $(-1)^j = (-1)^{j'}$, then $\pi^{-1}(j'+1)$ is also between $\pi^{-1}(j)$ and $\pi^{-1}(j+1)$. An alternative geometric description is the following: consider a C^1 Jordan curve $\mathcal{S}$ which intersects the horizontal axis transversely and at precisely N locations, numbered $k = 1, \dots, N$ in increasing order. Also number the same intersections successively along the curve $\mathcal{S}$. The second numbering j provides a permutation $j = \pi(k)$, relative to the first. Any permutation π arising by such a construction is called meander permutation. See Fig. 3 for an example of a dissipative Morse meander $\pi \in S_{13}$. For many more examples see [24].

It is fairly straightforward to see that Sturm permutations $\pi = \pi_f$ are dissipative Morse meanders. In fact, $v_1 = \underline{v}$ and $v_N = \bar{v}$ are the lowest and highest equilibria in the global attractor $\mathcal{A}_f$ as discussed in Section 1. In particular (2.2), (2.3) imply $\pi(1) = 1$ and $\pi(N) = N$. The Morse property of π follows because $i_j = i(v_j)$ are the Morse indices of the equilibria v_j, by [28], and hence nonnegative. In particular $i_N = 0$ for the top sink $\bar{v} = v_N$, and hence N is odd by (2.5) mod 2 with $j = N$. The meander property follows by shooting: consider the equilibrium second order ODE (1.5) with initial condition $v_x = 0$ given by the horizontal v-axis in the (v, v_x) phase plane. The diffeomorphic image of the v-axis in the phase plane (v, v_x), at $x = 1$, is called the *shooting curve* $\mathcal{S}$. The curve $\mathcal{S}$ crosses the v-axis transversely, at the boundary values $v_j(x)$ of the hyperbolic equilibria evaluated at $x = 1$. The permutation π associated to the shooting curve $\mathcal{S}$ is the Sturm permutation defined in (2.3), (2.4) above. Numbers j above the v-axis indeed

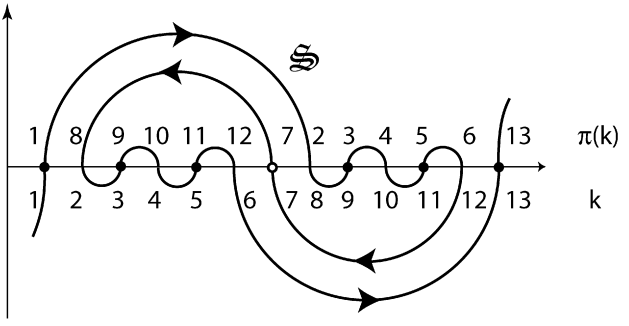

Fig. 3. Dissipative Morse meander permutations $\pi = (1, 8, 9, 10, 11, 12, 7, 2, 3, 4, 5, 6, 13)$ and shooting curve $\mathcal{S}$. For k below the horizontal axis, $j = \pi(k)$ is denoted above. Filled dots indicate $i_j = 0$ and the circled dot has $i_7 = 2$. For all other intersections, $i_j = 1$.

indicate the ordering of equilibria at $x = 0$, i.e., along the shooting curve $\mathcal{S}$, whereas numbers k below the axis indicate their ordering at $x = 1$. This explains why Sturm permutations are dissipative Morse meanders. It is significantly more difficult, but has been established in [21], that all dissipative Morse meanders π are indeed Sturm permutations $\pi = \pi_f$, for some nonlinearity f.

The precise numbering of equilibria is just a minor issue of bookkeeping, but also a major source of confusion. Let us clarify. In Fig. 3, numbers j *above* the horizontal axis indicate the label of the equilibrium v_j which is defined by the intersection point of the shooting curve $\mathcal{S}$ with the horizontal axis. This assumes that equilibria are ordered by increasing index j, at $x = 0$, according to the convention $h_0 = \mathrm{id}$ underlying (2.4). Let k denote the number at j, but *below* the horizontal axis. Then the values $v_{h_0(j)} = v_j$ are ordered as the k are, at $x = 1$, by definition (2.2) of h_0. On the other hand, the values $v_{h_1(k)}$ are also ordered as the k themselves are, at $x = 1$, by definition (2.2) of h_1. Therefore $j = h_0(j) = h_1(k)$. In particular $j = h_0^{-1}(h_1(k)) = \pi(k)$, as claimed in Fig. 3.

In [22] it has been shown that Sturm attractors $\mathcal{A}_f$ and $\mathcal{A}_g$ are C^0 orbit equivalent if their Sturm permutations coincide:

$$\pi_f = \pi_g \quad \Rightarrow \quad \mathcal{A}_f \cong \mathcal{A}_g. \tag{2.6}$$

Here C^0 orbit equivalence $\cong$ requires that there exist a homeomorphism between $\mathcal{A}_f$ and $\mathcal{A}_g$ which maps orbits of the PDE (1.1), (1.2) under nonlinearity f to orbits under g, preserving time direction. As we shall see and discuss below, the converse of (2.6) does not always hold.

The key to our construction of prescribed connection graphs $\mathcal{C}_f = G_2$ from boundary *ZS*-Hamiltonian pairs (h_0, h_1) between $\underline{v}$ and $\bar{v}$ in G_2 will be the derivation of connection graphs $\mathcal{C}_f$ from Sturm permutations π_f. We present these results following [20]; see also the elegant form due to [49].

One central ingredient to determining $\mathcal{C}_f$ from π_f is the notion of blocking. Let v, v_1, v_2 be three distinct equilibria in $\mathcal{A}$. We say that v *blocks* any heteroclinic orbit $v_1 \rightsquigarrow v_2$, if one of the following two conditions holds:

$$z(v_1 - v) < z(v_2 - v), \quad \text{or} \tag{2.7}$$

$$z(v_1 - v) = z(v_2 - v) \quad \text{and } v \text{ is between } v_1 \text{ and } v_2 \text{ at } x = 0 \text{ or } x = 1. \tag{2.8}$$

Indeed blocking prevents heteroclinic orbits $u(t, \cdot)$ from v_1 to v_2 by the Sturm nodal property (1.9) of nonincreasing $t \mapsto z(u(t, \cdot) - v)$.

For later reference and as an introduction to blocking, we mention the following useful blocking lemma.

Lemma 2.1. *Let v_1, v_2, v_3, v_4 be distinct equilibria such that $v_4 \rightsquigarrow v_3$ and $v_2 \rightsquigarrow v_1$. Assume that the following overlap conditions hold, either all at $x = 0$ or all at $x = 1$: the equilibrium v_2 is between v_3, v_4, and v_3 is between v_1, v_2. Then*

$$z(v_4 - v_2) \geqslant z(v_3 - v_1) + 2. \tag{2.9}$$

Proof. Since v_2 between v_3, v_4 does not block $v_4 \rightsquigarrow v_3$, blocking conditions (2.7), (2.8) must both be violated for the triple v_2, v_3, v_4. Therefore

$$z(v_4 - v_2) > z(v_3 - v_2). \tag{2.10}$$

Similarly, v_3 between v_1, v_2 does not block $v_2 \rightsquigarrow v_1$ and therefore

$$z(v_2 - v_3) > z(v_1 - v_3). \tag{2.11}$$

Together, (2.10) and (2.11) prove the lemma. □

Due to cascading, we only have to consider equilibria v_1, v_2 of adjacent Morse indices $i(v_1) = i$ and $i(v_2) = i + 1$ as candidates for adjacency in the connection graph $\mathcal{C}_f$. For such *Morse adjacent* pairs we can refine the notion of blocking. By Morse–Smale transversality of stable and unstable manifolds, a unique heteroclinic orbit $u(t, x)$ may run from v_2 to v_1, but not vice versa. The dropping property of the zero number z on $X \setminus \{0\}$ implies for a heteroclinic orbit $u(t) \in X$ from v_2 to v_1 that

$$\begin{aligned} i = \operatorname{codim} W^s(v_1) &\leqslant z\big(u(t) - v_1\big) \leqslant z(v_2 - v_1) \\ &= z(v_1 - v_2) \leqslant z\big(u(t) - v_2\big) < \dim W^u(v_2) = i + 1. \end{aligned} \tag{2.12}$$

See (1.10) and [1,8,34] for the first and last inequality. Therefore we may also assume $z(v_1 - v_2) = i$. We say that an equilibrium $v \in \mathcal{C}_f$ *i-blocks* v_1, v_2 if

$$\begin{aligned} &z(v - v_1) = z(v - v_2) = z(v_1 - v_2) = i = i(v_1) = i(v_2) - 1 \quad \text{and} \\ &\quad v(x) \text{ is between } v_1(x) \text{ and } v_2(x) \text{ at } x = 0 \text{ or, equivalently, at } x = 1. \end{aligned} \tag{2.13}$$

Obviously i-blocking prevents heteroclinic orbits $u(t)$ between v_1 and v_2, by z-dropping of $z(u(t) - v)$.

Theorem 2.2. *(See [20].) Let v_1, v_2 be hyperbolic equilibria in $\mathcal{A}_f$ numbered such that $i(v_1) \leqslant i(v_2)$. Then v_1, v_2 are connected by an edge in the connection graph $\mathcal{C}_f$, i.e., by a heteroclinic orbit $v_2 \rightsquigarrow v_1$, if, and only if, there exists a nonnegative integer i such that the following two properties hold*:

(i) $z(v_1 - v_2) = i(v_1) = i(v_2) - 1 = i$, *and*
(ii) v_1, v_2 *are not i-blocked.*

The above theorem provides an explicit algorithm

$$\pi_f \mapsto \mathcal{C}_f \tag{2.14}$$

which determines the connection graph $\mathcal{C}_f$ from the Sturm permutation π_f, once the Morse indices $i_k = i(v_k)$ and the zero numbers $z(v_j - v_k)$ are known, for all $1 \leqslant j, k \leqslant N$. We combine these numbers in the *z-matrix* with entries

$$z_{jk} := \begin{cases} i(v_k) = i_k & \text{for } j = k, \\ z(v_j - v_k) = z(v_k - v_j) & \text{for } j \neq k. \end{cases} \tag{2.15}$$

An explicit expression for the diagonal entries i_k in terms of $\pi = \pi_f$ was given in (2.5). The off-diagonal entries $z_{jk} = z_{kj}$, for $1 \leqslant j < k \leqslant N$ satisfy

$$z_{jk} = i_j + \frac{1}{2}\big((-1)^k \operatorname{sign}\big(\pi^{-1}(k) - \pi^{-1}(j)\big) - 1\big) + \sum_{j<\ell<k} (-1)^\ell \operatorname{sign}\big(\pi^{-1}(\ell) - \pi^{-1}(j)\big), \tag{2.16}$$

again with empty sums denoting zero. See [20,28,44]. For practical purposes we also mention the following properties, for all $1 \leqslant j < N$ and, in the last line, $1 \leqslant j < k < N$:

$$z_{11} = i_1 = z_{NN} = i_N = 0, \tag{2.17}$$

$$z_{j1} = z_{jN} = 0, \tag{2.18}$$

$$z_{j,j+1} = \min\{i_j, i_{j+1}\}, \tag{2.19}$$

$$z_{j,k+1} = z_{jk} + \frac{1}{2}\big((-1)^{k+1} \operatorname{sign}\big(\pi^{-1}(k+1) - \pi^{-1}(j)\big) + (-1)^k \operatorname{sign}\big(\pi^{-1}(k) - \pi^{-1}(j)\big)\big). \tag{2.20}$$

In Fig. 4 we collect the 18 connection graphs $\mathcal{C}_f$ of Sturm attractors $\mathcal{A}_f$ with $N = 9$ hyperbolic equilibria. Trivially isomorphic copies by $\pi \mapsto \pi^{-1}$, as generated by $x \mapsto -x$, and by conjugation with the flip $\sigma = (N, N-1, \ldots, 2, 1)$, as generated by $v \mapsto -v$, are omitted. See [16].

Corollary 2.3. *Let v_j, v_k be equilibria with, among all equilibria from $\mathcal{C}_f$, adjacent boundary values at $x = 0$ or at $x = 1$. Then v_j, v_k are adjacent in the connection graph $\mathcal{C}_f$, i.e., $v_j \rightsquigarrow v_k$ or $v_k \rightsquigarrow v_j$.*

Proof. Equilibria v_j, v_k with adjacent boundary values cannot be i-blocked, for any i. By Theorem 2.2 it only remains to check property (i) for v_j, v_k. Reflecting $x \mapsto 1 - x$ and $v \mapsto -v$, if necessary, we may assume adjacency of the boundary values at $x = 0$, i.e., $k = j + 1$. Then $i(v_k) = i(v_j) \pm 1$, by (2.5), and (2.19) implies property (i) for v_j, v_k. This proves the corollary. □

By Corollary 2.3, we always have two boundary Hamiltonian paths h_0 and h_1 in our connection graph $\mathcal{C}_f$. The two paths are given by the succession of vertices $v_k \in \mathcal{E}$, ordered by their boundary values at $x = 0$ and $x = 1$, respectively. In our present notation, specifically, the paths are

$$\begin{aligned} h_0&: \quad v_1 v_2 \ldots v_N, \\ h_1&: \quad v_{\pi(1)} v_{\pi(2)} \ldots v_{\pi(N)}. \end{aligned} \tag{2.21}$$

Clearly these paths arise from the permutations $h_0 = \mathrm{id}$ and $h_1 = \pi$ defined via the boundary ordering of equilibria in (2.2). The paths start and end at the boundary of $\mathcal{C}_f$ because $v_1 = \underline{v}$ and $v_N = \bar{v}$ are on the boundary of the L^2-orthogonal Sturm–Liouville projection $P\mathcal{A}_f$ discussed in Section 1, (1.10).

None of the above results uses planarity of $P\mathcal{A}_f$. Our proof of the remaining converse parts of Theorems 1.1, 1.2, will show how boundary ZS-Hamiltonian pairs (h_0, h_1) in filled graphs G_2,

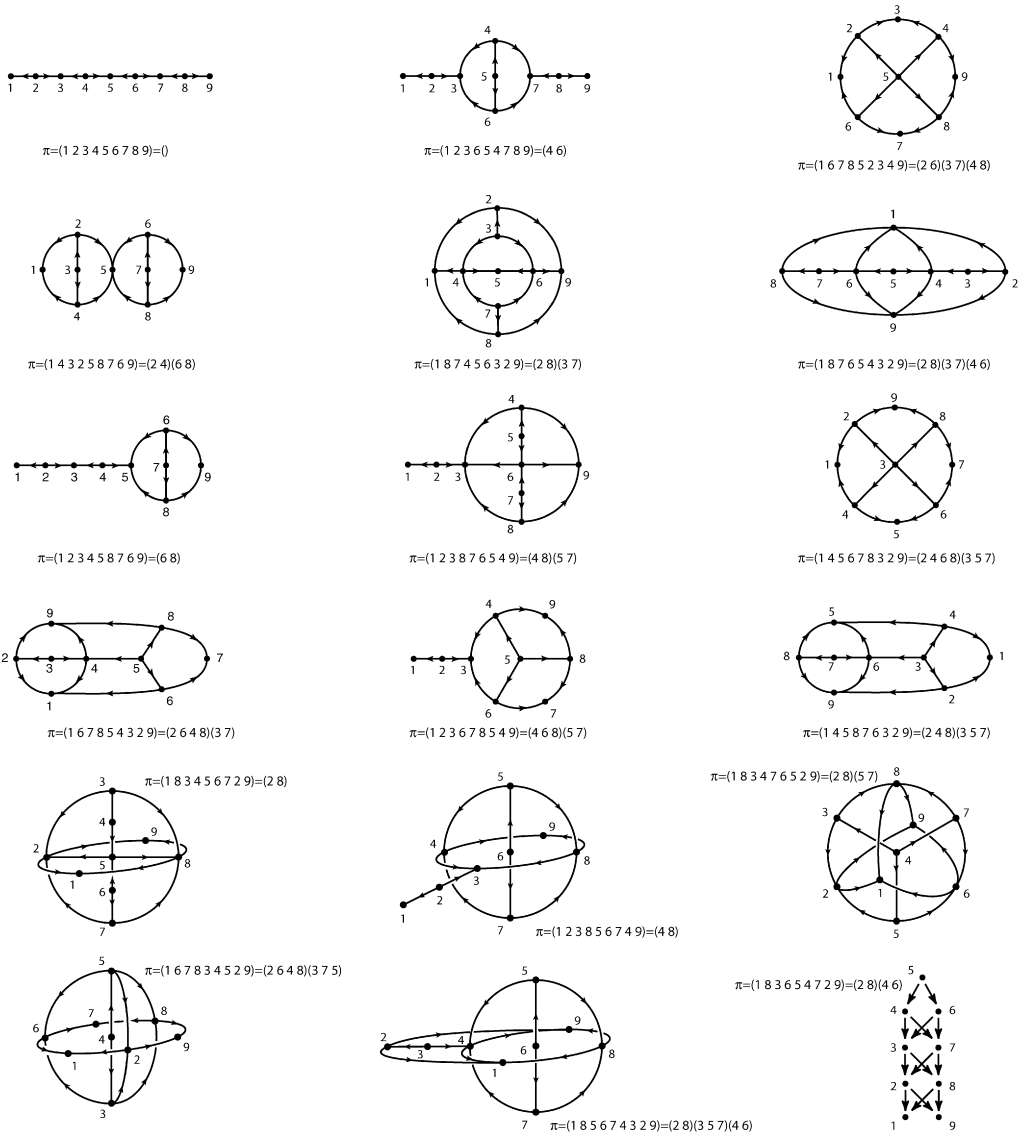

Fig. 4. All 18 connection graphs $\mathcal{C}_f$ of Sturm attractors $\mathcal{A}_f$ with $N = 9$ equilibria, up to trivial isomorphisms generated by $\pi \mapsto \pi^{-1}$ and $\pi \mapsto \sigma\pi\sigma^{-1}$ with $\sigma = (9, 8, \ldots, 2, 1)$. Equilibria are numbered such that $h_0 = \mathrm{id}$.

viewed as permutations of the equilibrium labels $1, \ldots, N$, will give rise to dissipative Morse meander permutations $\pi := h_0^{-1} h_1$ with prescribed connection graph $\mathcal{C}_f = G_2$.

3. Example: *n*-gon attractors

In this section we pause for a moment to illustrate our approach with a specific class of examples: n-gon attractors $\mathcal{A}_{n,m}$ for $1 \leqslant m < n$. See Fig. 2 for the cases $1 \leqslant n/2 \leqslant m < n \leqslant 6$ and Fig. 5 for the general cases $\mathcal{A}_{n,n-1}$ and $\mathcal{A}_{n,n-[n/2]}$ where $[\cdot]$ denotes the floor function.

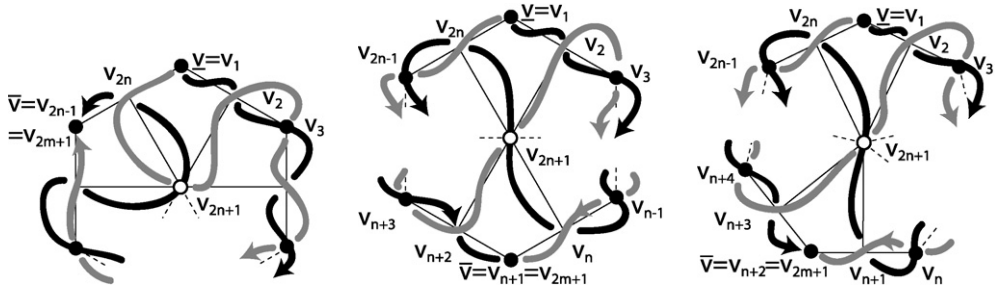

(a) $m = n - 1$ (b) $m = n/2$ (c) $m = (n + 1)/2$

Fig. 5. The n-gon attractors $\mathcal{A}_{n,m}$ with (a) $m = n - 1$; (b) n even and $m = n/2$; (c) n odd and $m = (n + 1)/2$. Z-Hamiltonian path h_0 (solid) and S-Hamiltonian path h_1 (gray).

The 1-skeleton G of the n-gon attractor is a regular plane n-gon with Morse sink vertices v_k labeled $k = 1, 3, \ldots, 2n - 1$, clockwise. The filled graph G_2 possesses the additional Morse saddles $2k$ bisecting the edges $\{2k - 1, 2k + 1\}$, for $1 \leqslant k < n$, and the edge $\{2n - 1, 1\}$ for $k = n$. The barycenter of the n-gon is the Morse source $2n + 1$ of G_2, connected by edges to each Morse saddle. Obviously there is only one bounded face F: the interior of the n-gon. The boundary ∂F is the 1-skeleton G.

The acyclic orientations of G, without di-sources and di-sinks other than the Morse sinks $\underline{v}$ and $\bar{v}$, are characterized by the positions of $\underline{v}$ and $\bar{v}$ along the boundary n-gon ∂F: the two n-gon segments between $\underline{v}$ and $\bar{v}$ are oriented from $\underline{v}$ to $\bar{v}$. Without loss of generality we label

$$\underline{v} = v_1, \qquad \bar{v} = v_{2m+1} \tag{3.1}$$

for some $1 \leqslant m < n$.

We have seen in [23] how any planar Sturm attractor $\mathcal{A}_f$ possesses such an orientation. Conversely, we now construct dissipative Morse meander permutations $\pi \in S_{2n+1}$ such that $\pi = \pi_f$ implies $\mathcal{C}_f = G_2$, for our n-gon. In view of Theorem 1.3 it will be sufficient to show that the 1-skeletons coincide:

$$\mathcal{C}_f^1 = G. \tag{3.2}$$

To construct π we follow the program outlined in Section 1 and at the end of Section 2, based on the above orientation of G with di-source $\underline{v} = v_1$ and di-sink $\bar{v} = v_{2m+1}$. Properties (a)–(c) of Z-Hamiltonian paths h_0 from $\underline{v}$ to $\bar{v}$, as specified in Section 1, identify the path $h_0 = v_{h_0(1)} v_{h_0(2)} \ldots v_{h_0(N)}$ with $N = 2n + 1$ to be given uniquely by the permutation

$$h_0 = \begin{pmatrix} 1 & 2 & 3 & \ldots & 2m & 2m+1 & 2m+2 & 2m+3 & \ldots & 2n & 2n+1 \\ 1 & 2 & 3 & \ldots & 2m & 2n+1 & 2n & 2n-1 & \ldots & 2m+2 & 2m+1 \end{pmatrix} \tag{3.3}$$

of the equilibrium labels. Similarly, the unique S-Hamiltonian path from $\underline{v}$ to $\bar{v}$ is given by the permutation

$$h_1 = \begin{pmatrix} 1 & 2 & \ldots & 2(n-m) & 2(n-m)+1 & 2(n-m)+2 & \ldots & 2n & 2n+1 \\ 1 & 2n & \ldots & 2m+2 & 2n+1 & 2 & \ldots & 2m & 2m+1 \end{pmatrix}, \tag{3.4}$$

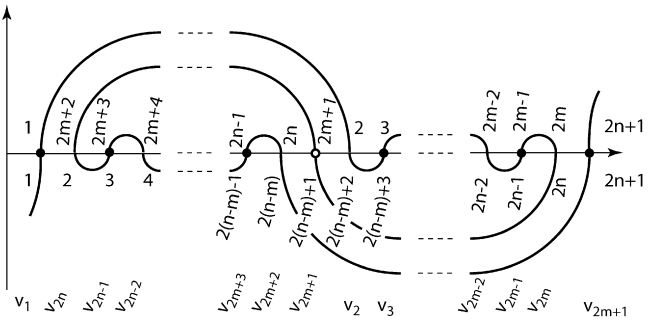

Fig. 6. Shooting curve and Morse indices of $\pi_{n,m}$. Below axis: k; above axis: $\pi_{n,m}(k)$. Note that labels j above and k below axis indicate equilibrium $v_{h_0(j)}$ and $v_{h_1(k)}$ in Fig. 5, respectively.

By recipe (2.3) this defines the candidate $\pi_{n,m} := h_0^{-1} \circ h_1$ for a Sturm permutation with Sturm attractor $\mathcal{A}_{n,m}$ and connection graph $\mathcal{C}_{n,m} = G_2$ to be

$$\pi_{n,m} = \begin{pmatrix} 1 & 2 & \dots & 2(n-m) & 2(n-m)+1 & 2(n-m)+2 & \dots & 2n & 2n+1 \\ 1 & 2m+2 & \dots & 2n & 2m+1 & 2 & \dots & 2m & 2n+1 \end{pmatrix}. \tag{3.5}$$

Note the symmetry under $m \mapsto n-m$:

$$\pi_{n,n-m} = \pi_{n,m}^{-1}. \tag{3.6}$$

It is straightforward to check that the permutation $\pi_{n,m}$ is a dissipative Morse meander. See Fig. 6 for the shooting curve and the Morse indices i_k of $\pi_{n,m}$.

To show that the connection graph $\mathcal{C}_{n,m}$ of the Sturm permutation $\pi_{n,m} = \pi_f$ is the filled n-gon G_2 it remains to check that the 1-skeleton $\mathcal{C}^1_{n,m}$ coincides with the n-gon boundary G; see (3.2). More specifically, we have to show that the saddle v_{2k} indeed connects to v_{2k-1} and v_{2k+1}, for $k = 1, \dots, n$, and to no other sinks. Subscripts are taken mod $2n$ here. This is a case of checking for heteroclinic orbits with $i = 0$, by Theorem 2.2.

We first show $v_{2k} \rightsquigarrow v_{2k\pm1}$. Indeed v_{2k} and $v_{2k\pm1}$ are successors along the Hamiltonian paths h_0 or h_1. Hence their boundary values are adjacent at the boundary $x = 0$ or $x = 1$, among all equilibria. Therefore $i = 0$ blocking cannot occur. Moreover $i(v_{2k}) = 1$, $i(v_{2k\pm1}) = 0$, and hence $z(v_{2k} - v_{2k\pm1}) = \min\{i(v_{2k}), i(v_{2k\pm1})\} = 0$ by property (2.12) of the z-matrix. This proves $v_{2k} \rightsquigarrow v_{2k\pm1}$, by Theorem 2.2.

To exclude all other heteroclinic orbits $v_{2k} \rightsquigarrow v_{2j+1}$, $j \notin \{k-1, k\}$, we group the relevant indices k, j into two different sets L and R for the left and right arcs of the n-gon, oriented downward from $\underline{v}$ to $\bar{v}$:

$$L = \{2m+2, \dots, 2n\}, \qquad R = \{2, \dots, 2m\}. \tag{3.7}$$

Note that $v_{2k} \rightsquigarrow v_{2j+1}$ is 0-blocked by $v_{2k\pm1}$, within the same set and including $\underline{v}, \bar{v}$, because the orientation on each of these arcs, respectively, defines a total order with strict ordering of all

these equilibria on the whole interval $0 \leqslant x \leqslant 1$, and not just on the boundaries. Heteroclinic orbits $v_{2k} \rightsquigarrow v_{2j+1}$ with saddle v_{2k} and sink v_{2j+1} in different sets are excluded, because

$$z(v_{2k} - v_{2j+1}) \geqslant 1 \tag{3.8}$$

in that case. Indeed note that the boundary values of equilibria in L are strictly above those of R, at $x = 0$; see the ordering defined by h_0 in (3.3). The ordering at the other boundary, $x = 1$ is the reverse: L is below R. This proves (3.8). See also Fig. 8 below.

Summarizing, the 1-skeleton $\mathcal{C}^1_{n,m}$ of the connection graph $\mathcal{C}_{n,m}$ of the global attractor $\mathcal{A}_f = \mathcal{A}_{n,m}$ with Sturm permutation $\pi_{n,m}$ is indeed the prescribed n-gon, as was claimed in (3.2). Moreover the boundary orders of equilibria at $x = 0, 1$ are as was prescribed by the boundary *ZS*-Hamiltonian pair (h_0, h_1) from $\underline{v} = v_1$ to $\bar{v} = v_{2m+1}$ specified in (3.3), (3.4).

4. Example: *n*-gon faces in planar Sturm attractors

In the previous section we have studied the n-gon Sturm attractors $\mathcal{A}_{n,m}$ for $1 \leqslant m < n$, which consist of just a single face F with one source w inside, and n sink-saddle pairs on its n-gon boundary ∂F. In the present section we study an arbitrary face F, alias the unstable manifold $W^u(w)$ of an arbitrary source w, of any planar Sturm attractor $\mathcal{A} = \mathcal{A}_f$ with Sturm permutation π_f. The face boundary ∂F must then be an n-gon, for some $n \geqslant 2$. This has already been observed in [23] and is contained in the "only if" part of Theorem 1.1: the 1-skeleton is cellular. The analysis of n-gon faces in the present section will therefore serve as a paradigm to our subsequent proof, in Section 5, that boundary *ZS*-Hamiltonian pairs (h_0, h_1) in a plane filled graph G_2 indeed give rise to a planar Sturm attractor $\mathcal{A} = \mathcal{A}_f$ with prescribed connection graph G_2, via the Sturm permutation $\pi_f = \pi := h_0^{-1} \circ h_1$.

The general environment in the shooting curve $\mathcal{S}$ of a source equilibrium $w = v_{2m+1}$ in any planar Sturm attractor $\mathcal{A}$ is sketched in Fig. 7. The shooting curve $\mathcal{S}$ consists of arcs above and below the horizontal axis $v(1)$ which match globally, at their end points, to form the Jordan curve $\mathcal{S}$. Consider $\mathcal{S}$ oriented from the lowest equilibrium sink $\underline{v}$ to the highest, $\bar{v}$. Then $\mathcal{S}$ crosses the v-axis transversely, by hyperbolicity. Crossings are upward, at equilibria v with even Morse index (here: sinks and sources), and are downward at odd Morse index (here: saddles). By (2.5) the Morse index increases by 1 along any arc which turns right, but decreases by 1 along left turning arcs.

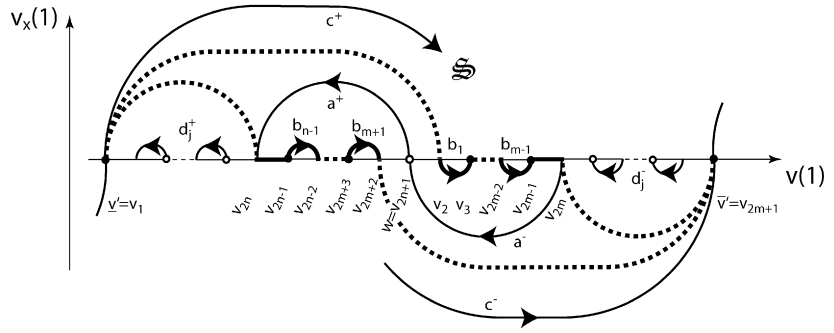

Fig. 7. Corona $v_1, \ldots, v_{2n}$ of a source $w = v_{2n+1}$ in the shooting curve $\mathcal{S}$ of a planar Sturm attractor $\mathcal{A}$. For notation see text. The face boundary ∂F of w is indicated by thick solid and dashed segments.

By these observations, the source $w = v_{2n+1}$ comes associated with the following *corona* of sinks and saddles. Let v_{2n}, below $w = v_{2m+1}$, denote the saddle end point of the shooting arc a^+ emanating from w to the left. Similarly, let v_{2m} be the saddle starting point, above w, of the shooting arc a^- from the right which terminates at w. Because $\mathcal{S}$ is a shooting curve, vertically neighboring arcs must have opposite orientation. In particular, the (possibly absent) upper arcs $b_{n-1}, \dots, b_{m+1}$ immediately below a^+ are oriented to the right and are right turning. Therefore they start at $n - m - 1$ sinks $v_{2n-1}, \dots, v_{2m+3}$ and terminate at $n - m - 1$ saddles $v_{2n-2}, \dots, v_{2m+2}$. This defines the integer $n - m - 1 \geqslant 0$. Similarly, we find $m - 1$ (possibly absent) right oriented and left turning lower shooting arcs $b_1, \dots, b_{m-1}$ immediately above a^-. These arcs start at saddles $v_2, \dots, v_{2m-2}$ and terminate at sinks $v_3, \dots, v_{2m-1}$. The numbers $m - 1$ and $n - m - 1$ of these arcs b_k, incidentally, define m, n with $1 \leqslant m < n$. Finally, let v_1 denote the starting point of the first shooting arc c^+ above a^+. Note that c^+ indeed exists and v_1 must be a sink. Analogously, the sink v_{2m+1} denotes the end point of the first shooting arc c^- below a^-. This defines the sink and saddle equilibria $v_1, \dots, v_{2n}$ in the Sturm attractor $\mathcal{A}$ which we call the corona of the source $w = v_{2n+1}$.

Theorem 4.1. *The equilibria $v_1, \dots, v_{2n+1}$ introduced above define an n-gon face F with source $w = v_{2n+1}$. The periphery is an n-gon ∂F with alternating sinks and saddles $v_1, \dots, v_{2n}$. The sink v_1 is a di-source, $\underline{v}' = v_1$, and the sink v_{2m+1} is a di-sink $\overline{v}' = v_{2m+1}$ on ∂F, as described geometrically in Section 3. Specifically we claim that the saddles $v_2, \dots, v_{2n}$ and the source v_{2n+1} only possess the following heteroclinic connections to sinks and saddles, respectively*:

(i) $v_{2n+1} \rightsquigarrow v_{2k}$, *for* $k = 1, \dots, n$;
(ii) $v_{2k} \rightsquigarrow v_{2k-1}$, *for* $k = 1, \dots, n$;
(iii) $v_{2k} \rightsquigarrow v_{2k+1}$, *for* $k = 1, \dots, n-1$;
(iv) $v_{2n} \rightsquigarrow v_1$.

In particular the connection graph $\mathcal{C}_f$ is the filled graph of its 1-skeleton $\mathcal{C}_f^1$.

We split the proof of Theorem 4.1 into the string of Lemmas 4.2–4.6 below. Lemma 4.2 establishes $v_{2k} \rightsquigarrow v_{2k-1}$ as in (ii), except for $k = 1, m+1$. Similarly, it takes care of (iii), except for $k = m$. In Lemma 4.3 we establish the connections from the source $w = v_{2n+1}$ to the periphery v_{2k} as claimed in (i). The case $k = 1$ of (ii), which leads to the di-source $\underline{v}' = v_1$ on ∂F, is addressed in Lemma 4.4, together with claim (iv). The remaining cases $k = m$, $m+1$ lead to the di-sink $\overline{v}' = v_{2m+1}$ on ∂F, in Lemma 4.5. Lemma 4.6 establishes the absence of further heteroclinic orbits from the source and saddles of F to adjacent Morse levels, and thus completes the proof of the theorem.

All lemmas in this section employ the notation and assumptions of the theorem.

Lemma 4.2.

$$v_{2k} \rightsquigarrow v_{2k-1} \quad \text{for } 1 < k \leqslant m \text{ or } m+1 < k \leqslant n, \tag{4.1}$$

$$v_{2k} \rightsquigarrow v_{2k+1} \quad \text{for } 1 \leqslant k < m \text{ or } m+1 \leqslant k < n. \tag{4.2}$$

In particular the equilibria $v_k(x)$ are ordered as follows, pointwise for all $0 \leqslant x \leqslant 1$:

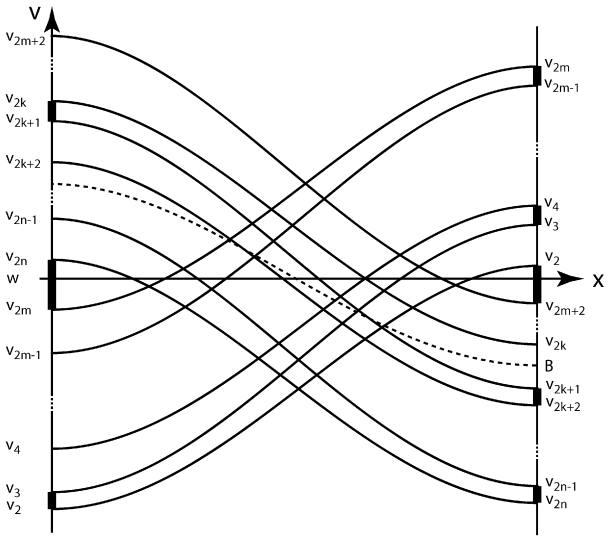

Fig. 8. Orderings of $v_k(x)$ in general face F. Hashed regions at $x = 0, 1$ indicate adjacency of equilibria.

$$v_2 < v_3 < v_4 < \cdots < v_{2m}, \tag{4.3}$$

$$v_{2m+2} > v_{2m+3} > v_{2m+4} > \cdots > v_{2n}. \tag{4.4}$$

At the boundaries the orders are

$$v_2 < v_3 < \cdots < v_{2m} < w = v_{2n+1} < v_{2n} < \cdots < v_{2m+3} < v_{2m+2} \quad \text{at } x = 0, \quad \text{and} \tag{4.5}$$

$$v_{2n} < v_{2n-1} < \cdots < v_{2m+2} < w = v_{2n+1} < v_2 < \cdots < v_{2m-1} < v_{2m} \quad \text{at } x = 1. \tag{4.6}$$

See Fig. 8 for an illustration of Lemma 4.2. Without loss of generality we have normalized to the case $w = v_{2n+1} \equiv 0$.

Proof. We only consider the claims for $m+1 \leqslant k \leqslant n$. Substituting $v \mapsto -v$ the cases $1 \leqslant k \leqslant m$ are analogous and will be omitted.

At $x = 1$ and for $m + 1 < k \leqslant n$, the sink v_{2k-1} is adjacent to its preceding saddle v_{2k} along the v-axis; see Fig. 7. By Corollary 2.3 this shows $v_{2k} \rightsquigarrow v_{2k-1}$ for $m + 1 < k \leqslant n$ and hence proves claim (4.1). Because $i(v_{2k}) = 1$ at the saddles, the heteroclinic orbit also implies $z(v_{2k} - v_{2k-1}) = 0$, which shows half of the ordering (4.4). Similarly, Corollary 2.3 implies $v_{2k} \rightsquigarrow v_{2k+1}$ for $m + 1 \leqslant k < n$, because the sink v_{2k+1} is adjacent to the subsequent saddle v_{2k} along the shooting curve $\mathcal{S}$ and at $x = 0$. This proves claim (4.2) and the remaining half of (4.4). Claims (4.5) and (4.6) follow from the respective boundary orders of v_{2m}, v_{2n+1}, v_{2n} and from (4.3), (4.4). This proves the lemma. □

Lemma 4.3.

$$w = v_{2n+1} \rightsquigarrow v_{2k}, \quad \text{for } k = 1, \ldots, n. \tag{4.7}$$

Proof. The equilibria v_2 and v_{2m+2} are adjacent to the F-source $w = v_{2n+1}$ at $x = 1$, by Fig. 7. Also by Fig. 7, the shooting arcs $a^{\pm}$ of the F-source $w = v_{2n+1}$ reach to v_{2m} and v_{2n}, which implies adjacency at $x = 0$. By Corollary 2.3 this shows the four heteroclinic connections

$$v_{2n+1} \rightsquigarrow v_2, v_{2m}, v_{2m+2}, v_{2n}. \tag{4.8}$$

Interchanging the roles of a^+ and a^- by the substitution $v \mapsto -v$, if necessary, we consider the arc a^+ and only show $v_{2n+1} \rightsquigarrow v_{2k}$ for $m+1 < k < n$, without loss of generality.

We proceed by induction on k, starting at the settled case $k = m+1$. We thus assume $v_{2n+1} \rightsquigarrow v_{2k}$ has been proved. We now show indirectly

$$v_{2n+1} \rightsquigarrow v_{2k+2}. \tag{4.9}$$

If the heteroclinic orbit (4.9) does not exist, then it is i-blocked with $i = 1$ by some other equilibrium B; see Theorem 2.2. Indeed $i(v_{2n+1}) = 2$ and $i(v_{2k+2}) = 1$. Moreover $z(v_{2n+1} - v_{2k+2}) < \dim \mathcal{A} = 2$, by (1.10), and $z(v_{2n+1} - v_{2k+2}) \geqslant 1$ by the boundary orderings (4.5), (4.6). Therefore $z(v_{2n+1} - v_{2k+2}) = 1$ and B exists, supposedly. To reach a contradiction and thus complete the induction step (4.9) we show below that

$$z(v_{2k} - B) = 0 < 1 = z(v_{2k+1} - B). \tag{4.10}$$

Then B blocks $v_{2k} \rightsquigarrow v_{2k+1}$, by (2.7), in contradiction to Lemma 4.2.

To prove the present lemma it therefore remains to show (4.10). Again from (1.10) we recall $z(v - B) < \dim \mathcal{A} = 2$ for all equilibria v. The zero numbers in (4.10) can therefore be determined from the boundary values at $x = 0, 1$.

Because B is assumed to be 1-blocking for $w = v_{2n+1} \rightsquigarrow v_{2k+2}$, say at $x = 1$, we have $v_{2k+2} < B < w$ at $x = 1$. Because v_{2k+1} and v_{2k+2} are adjacent, at $x = 1$, this implies

$$v_{2k+2} < v_{2k+1} \leqslant B < w \quad \text{at } x = 1; \tag{4.11}$$

see also (4.6). Moreover $z(w - B) = z(v_{2k+2} - B) = 1$, by 1-blocking, and therefore

$$w < B < v_{2k+2} < v_{2k+1} < v_{2k} \quad \text{at } x = 0; \tag{4.12}$$

see also (4.5). Together this proves $B \neq v_{2k+1}$ and $z(v_{2k+1} - B) = 1$. By induction hypothesis $w \rightsquigarrow v_{2k}$, however, B does not block $w \rightsquigarrow v_{2k}$. Therefore $z(w - B) = 1$ and (4.12) imply that $z(v_{2k} - B) \in \{0, 1\}$ must be zero. This proves (4.10), the induction step (4.9), and the lemma. □

As a preparation for Lemma 4.4 we define the two candidates $\underline{v}_2$ and $\underline{v}_{2n}$ for $\underline{v}' = v_1$ as follows. The saddles v_2, v_{2n} each possess an unstable manifold with two heteroclinic orbits. One of these, running upward at any fixed $0 \leqslant x \leqslant 1$, terminates at v_3, v_{2n-1}, respectively; see Lemma 4.2. The other one, running downward, terminates at equilibria which we call $\underline{v}_2, \underline{v}_{2n}$, respectively. In other words:

$$v_2 \rightsquigarrow \underline{v}_2 < v_2, \tag{4.13}$$

$$v_{2n} \rightsquigarrow \underline{v}_{2n} < v_{2n}. \tag{4.14}$$

The following lemma closes the (undirected) boundary cycle ∂F at v_1.

Lemma 4.4.

$$\underline{v}_2 = \underline{v}_{2n} = v_1. \tag{4.15}$$

In particular $v_2 \rightsquigarrow v_1$ *and* $v_{2n} \rightsquigarrow v_1$.

Proof. We recall that v_1 is the left starting point of the first shooting arc c^+ above the arc a^+ from $w = v_{2n+1}$ to v_{2n}; see Fig. 7.

Between v_1 and v_{2n} there are (possibly absent) arcs d_j^+ below c^+ which connect sources to saddles. To identify $\underline{v}_{2n} = v_1$ we first invoke the defining relation (4.14) of the downward heteroclinic orbit $v_{2n} \rightsquigarrow \underline{v}_{2n} < v_{2n}$. By Lemma 2.1 the target sink $\underline{v}_{2n}$ cannot be located below any of the arcs d_j on the $v(1)$-axis. Indeed (2.9) is impossible by $\dim \mathcal{A} = 2$. Likewise, $\underline{v}_{2n}$ cannot be located outside the arc c^+. Therefore $\underline{v}_{2n} = v_1$.

Similarly, Lemma 2.1 also implies $\underline{v}_2 = v_1$. The above argument indeed applies verbatim if we include the arc $d_0 := a^+$. This proves the lemma. □

Analogously to $\underline{v}_2$ and $\underline{v}_{2n}$ in (4.13), (4.14) we define $\bar{v}_{2m}$ and $\bar{v}_{2m+2}$ by the relations

$$v_{2m} \rightsquigarrow \bar{v}_{2m} > v_{2m}, \tag{4.16}$$

$$v_{2m+2} \rightsquigarrow \bar{v}_{2m+2} > v_{2m+2}. \tag{4.17}$$

The following lemma closes the (undirected) boundary cycle ∂F at v_{2m+1}.

Lemma 4.5.

$$\bar{v}_{2m} = \bar{v}_{2m+2} = v_{2m+1}. \tag{4.18}$$

In particular $v_{2m} \rightsquigarrow v_{2m+1}$ *and* $v_{2m+2} \rightsquigarrow v_{2m+1}$.

Proof. Substituting $v \mapsto -v$, this case is analogous to Lemma 4.4. □

Lemma 4.6. *The source* $w = v_{2n+1}$ *of* F *does not possess heteroclinic connections to any saddles besides* v_{2k}, $1 \leqslant k \leqslant n$. *The saddles* v_{2k}, $1 \leqslant k \leqslant n$, *do not possess any heteroclinic connections to any sinks besides* $v_{2k\pm1}$, *with indices taken* mod $2n$. *In particular* $\underline{v}' = v_1$ *and* $\bar{v}' = v_{2m+1}$ *on* ∂F.

Proof. In Lemmas 4.2, 4.4, 4.5 we have established two sink targets $v_{2k\pm1}$ for each saddle v_{2k}. Since the one-dimensional unstable manifolds of the saddles contain only two heteroclinic orbits, this proves the claim on saddles. That the source $w = v_{2n+1}$ does not connect to any saddles outside the corona $v_1, \ldots, v_{2n}$ follows from blocking Lemma 2.1, because $z(v - w) < \dim \mathcal{A} = 2$ for any equilibrium $v \in \mathcal{A}$, by (1.10). Indeed the closed circle ∂F of the corona heteroclinic orbits around w prevents any heteroclinic orbits from w crossing the corona.

Since v_1 and v_{2m+1} are the maximal and the minimal equilibrium in ∂F, by construction and in the boundary order at $x = 1$, this also proves $\underline{v}' = v_1$ and $\bar{v}' = v_{2m+1}$. This completes the proof of the lemma, and of Theorem 4.1. □

5. From *ZS*-Hamiltonian pairs and skeleton orientations to Sturm attractors

In this section we complete the proof of Theorems 1.2 and 1.1 on the characterization of the connection graphs $\mathcal{C}_f$ and their 1-skeletons $\mathcal{C}_f^1$ as filled graphs G_2 with boundary *ZS*-Hamiltonian pairs (h_0, h_1) and their oriented 1-skeletons G, respectively. In Theorem 1.3 we have recalled the equivalence of the characterizing graph theoretic properties of G_2 and G. The equivalence proof was on the graph level, directly, and did not recur to any dynamical systems concepts like connection graphs of Sturm attractors. In Section 4 of [23] we showed how Sturm attractors induce an orientation of the 1-skeleton $\mathcal{C}_f^1$. This proved that $G := \mathcal{C}_f^1$ satisfies the characterizing properties of Theorem 1.1 and thus completed the "only if" part of Theorems 1.1 and 1.2. In the present section, finally, we show how the existence of boundary *ZS*-Hamiltonian pairs (h_0, h_1) in G_2 (and of a compatible orientation of G) with properties (i), (ii) of Theorems 1.2 (and 1.1) conversely provides a connection graph $\mathcal{C}_f$ which is isomorphic to G_2.

As announced in Sections 1 and 4, our proof starts from the paths h_0, h_1 and defines

$$\pi := h_0^{-1} \circ h_1; \tag{5.1}$$

see also (2.3), (2.6). In Lemma 5.1 we show that $\pi = \pi_f$ is indeed a Sturm permutation. Based on [20] it is sufficient to show that π is a dissipative Morse meander. Recall Section 2 for this terminology. To establish the graph isomorphism $\mathcal{C}_f \cong G_2$ of the connection graph $\mathcal{C}_f$ with the prescribed filled graph G_2 we observe that any realization of the Sturm permutation $\pi = \pi_f$ by boundary orders $\tilde{h}_0, \tilde{h}_1$ of equilibria associated to the specific nonlinearity f in the PDE (1.1), (1.2) just amounts to a relabeling of the equilibria $v_1, \ldots, v_N$ by some permutation $\sigma \in S_N$; see Lemma 5.2. This allows us to choose a labeling such that $h_j = \tilde{h}_j$ indeed provide the boundary orders of the equilibria at $x = j = 0, 1$, as required in (2.2). Lemma 5.3 then establishes that $\mathcal{C}_f$ and G_2 are indeed isomorphic, with the identity isomorphism on the vertices. This completes the proof of Theorem 1.2.

To complete the proof of Theorem 1.1, then, only Theorem 1.3 needs to be invoked. Indeed we then have the cycle of implications {Sturm} $\Rightarrow$ {Theorem 1.1(i), (ii)} $\Rightarrow$ {Theorem 1.2(i), (ii)} $\Rightarrow$ {Sturm}, by [23, Theorem 1.3], and the proof of the "if" part of Theorem 1.2 given below.

Throughout the present section we fix the setting of Theorem 1.2(i), (ii). Specifically, we are given a finite, connected, plane, cellular and loop-free multigraph G with two distinct Morse sinks $\underline{v}$, $\bar{v}$ in the boundary ∂G. Moreover, the filled graph G_2 with N vertices $v_1, \ldots, v_N$ possesses a *ZS*-Hamiltonian pair (h_0, h_1) of paths, both of which start and terminate at $\underline{v}$ and $\bar{v}$, respectively. We consider the paths $h_j \in S_N$ as permutations of the vertices and define $\pi := h_0^{-1} \circ h_1$ as in (5.1).

Lemma 5.1. *The permutation $\pi = h_0^{-1} \circ h_1 \in S_N$ is a Sturm permutation, i.e., π is a dissipative Morse meander.*

Proof. Without loss of generality let the vertices $v_1, \ldots, v_N$ of G_2 be labeled such that $v_1 = \underline{v}$ and $v_N = \bar{v}$. Then the paths h_j, $j = 0, 1$, both satisfy $h_j(k) = k$, for $k = 1, N$, because they both start and end at v_1, v_N. In particular

$$\pi(k) = k, \quad \text{for } k = 1, N, \tag{5.2}$$

is dissipative.

We show next that π is a meander permutation, i.e., can be described by a Jordan curve $\mathcal{S}$; see Fig. 3. In fact we will derive the topology of the shooting curve $\mathcal{S}$, and its transverse crossings of the horizontal axis, from the Hamiltonian paths h_0 and h_1 (including their edge parts) in G_2, respectively. For this purpose we disentangle the paths h_0 and h_1, wherever they run parallel or antiparallel along the same edge AB between vertices A and B. We consider the path h_0 as running from A to B.

To define disentanglement we briefly recall our concept of *duality*, a slight variant G^* of the standard *dual graph* of G, from [23]. Vertices of G^* inside ∂G are the Morse sources of the filled graph G_2 in the bounded faces of G. We replace the single vertex of the standard dual, representing the exterior of ∂G, by two vertices $\underline{v}^*$, $\bar{v}^*$ as follows. Edges e^* of G^* connect Morse sources of adjacent faces of G. We orient edges e^*, based on the oriented edge e which the adjacent faces share, such that the ordered pair (e^*, e) is oriented positively at the bisecting Morse saddle $\{v\} = e \cap e^*$. Then $\bar{v}^*$ terminates all edges e^* which point away from ∂G, to the outside, whereas $\underline{v}^*$ provides a start vertex for all edges e^* pointing toward ∂G from the outside. See also [24] for some realistic examples.

On the 1-skeleton G, the *ZS*-Hamiltonian paths h_0 and h_1 then follow the given orientation of the edges. On the dual skeleton G^*, however, the paths follow opposite orientations: h_0 respects the orientation defined above, whereas h_1 runs against it. In other words, let h_0 run from A to B. Then h_0 and h_1 both run from A to B, in parallel, if one of A, B is a Morse sink. If one of A, B is a Morse source, on the other hand, then h_1 runs from B to A, i.e., antiparallel to h_0.

We also assign the Morse types $0, 1, 2$ respectively, to any vertex which is a Morse sink, saddle, or source. The Morse types of A, B are adjacent. Here then is the *disentanglement rule*:

h_1 runs

- to the left of h_0, viewed along the edge AB, if A is of higher Morse type than B, and
- to the right, otherwise. (5.3)

See Fig. 9 for illustrations of all four cases. Our rendering of the *ZS*-Hamiltonian paths (h_0, h_1) in Figs. 2 and 5 already respected the disentanglement rule.

It is an easy but important exercise to check that the *ZS*-Hamiltonian paths h_0 and h_1 cross each other, due to the disentanglement rule, at each vertex other than $\underline{v}$, $\bar{v}$. At sources, for example, this follows from Fig. 5(a), even when $\underline{v}'$ and $\bar{v}'$ are adjacent sinks in G. The case of only two sinks on the face boundary is particularly noteworthy; see also Fig. 2 top left.

By our duality construction, path crossing at sinks follows from crossing at sources. Indeed, sinks other than $\underline{v}$, $\bar{v}$ become sources of the filled dual. Moreover, the disentanglement rule (5.3)

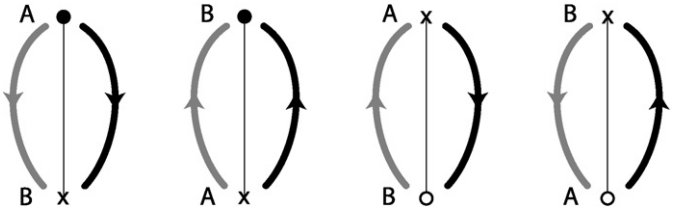

Fig. 9. Disentanglement of *ZS*-Hamiltonian paths h_0 (black) and h_1 (gray). Dots, crosses, and circles mark Morse sinks, saddles, and sources of Morse types 0, 1, and 2, respectively.

is invariant under interchange of sources with sinks and reversal of the path h_0. Since crossing is likewise invariant under reversal of both paths, this settles the case of sinks.

As a third example, we consider a path h_0 which leaves a face F and continues on the boundary ∂F. Crossing of h_0 and h_1 at the saddle then ensues because (h_0, h_1) is a *ZS*-pair. We leave the resulting not too few saddle cases to the reader.

For later reference we note that the disentangled oriented pair (h_0, h_1) defines a *negative orientation frame* at Morse sinks and Morse sources, but a *positive orientation frame* at Morse saddles. Graphically, this is indicated by over- and under-crossings of h_0. (In particular, we obtain an alternating knot by joining h_0 and the reverse of h_1.)

We now stretch the path h_1 by an orientation preserving homeomorphism H of the plane $\mathbb{R}^2$ to become the horizontal axis, oriented left to right from $\underline{v}$ to $\bar{v}$. The disentangled path h_0 then becomes a "shooting curve" $\mathcal{S} := H(h_0)$ which crosses the horizontal axis path $H(h_1)$ as required. Moreover $\pi = h_0^{-1} \circ h_1$ becomes the permutation associated to the Jordan curve $\mathcal{S}$, by construction. This proves that π is a meander.

Note that we do not claim that $\mathcal{S} = H(h_0)$ literally comes from an equilibrium ODE (1.5) with Neumann boundary conditions. But our construction certainly establishes the meander property of π.

For simplicity we henceforth consider the graph G_2 with paths h_0, h_1 as presented in the plane such that $H = \mathrm{id}$. We may then identify h_1 to be horizontal, and h_0 to coincide with the "shooting curve" $\mathcal{S}$.

To show that the permutation π is Morse we show, more specifically, that the Morse quantities i_k defined in (2.5) are not only all nonnegative but coincide with the Morse types of the vertices v_k. Here the vertices $v_1, \ldots, v_N$ are numbered along the path h_0, i.e., such that $h_0 = \mathrm{id} \in S_N$.

By the orientation of the frame (h_0, h_1) at any vertex of the horizontal path h_1, the shooting curve $\mathcal{S} = h_0$ crosses the horizontal axis upward, at Morse types 0, 2, and downward at Morse type 1. Consider an upward crossing at a Morse source w of Morse type 2. Then the arc of $\mathcal{S}$ emanating from w above the horizontal path h_1 terminates at a Morse saddle v^+ to the left of w. Indeed the orientation of the face boundary ∂F of w is compatible with h_0, h_1 and thus v^+ precedes w on h_1; see Figs. 2 and 5, as well as Section 2 in [23]. Similarly the w-arc of h_0 below h_1 emanates from a Morse saddle v^- and ends at w which precedes v^- on h_1. Along the arc $v^- w$ the path h_0 thus describes a right turn which increases the index i_k by 1, along with the Morse type. Along the arc wv^+ in h_0 both numbers are reduced by 1 through a left turn. See the explicit expression (2.5) for i_k.

A similar analysis applies to h_0 arcs between Morse saddles and Morse sinks to show that, again, the Morse type and the index i_k change by 1 in complete synchrony along the arcs.

By the Morse types in the filled graph G_2, any edge of the shooting path h_0 contains either Morse types 0, 1 or else 1, 2 as end points. Since $i_k = 0$ at the start vertex $\underline{v}$ of h_0, h_1, which is a Morse sink of type 0, we conclude that Morse types and i_k agree all along the Hamiltonian path h_0, i.e., on all vertices of the filled graph G_2. In particular the permutation π is also Morse, and the lemma is proved. □

In the above proof we have constructed a "shooting curve" $\mathcal{S} := H(h_0)$ as a homeomorphic image of the boundary Hamiltonian Z-path h_0 in the prescribed plane graph G_2. By [21] we now know that the abstract permutation $\pi := h_0^{-1} \circ h_1 = \pi_f$ is in fact a Sturm permutation and comes from a suitable nonlinearity f in the original PDE (1.1), (1.2). In particular we obtain an associated shooting curve $\mathcal{S}_f$ which, unlike the mock candidate $\mathcal{S}$, does arise from the equilibrium ODE (1.5) with Neumann boundary. The crossing directions of the horizontal axis, alias

the horizontal path h_1, coincide for both curves. We can, and will, therefore choose the plane homeomorphism such that $\mathcal{S} = \mathcal{S}_f$ is the shooting curve, itself.

Lemma 5.2. *Let $\pi = h_0^{-1} \circ h_1$ be the Sturm permutation $\pi = \pi_f$ associated to the boundary ZS-Hamiltonian pair (h_0, h_1) of the filled graph G_2, as in Lemma* 5.1. *Let h_j^f denote the boundary permutations of the equilibria $v_1, \dots, v_N$ of the PDE* (1.1), (1.2) *associated to the nonlinearity f, as in* (2.2). *Then there exists a permutation $\sigma \in S_N$ such that*

$$h_j^f = \sigma \circ h_j, \quad \text{for } j = 0, 1. \tag{5.4}$$

In other words, the equilibria can be relabeled by σ such that $h_j = h_j^f$ for $j = 0, 1$.

Proof. Let $\sigma := h_0^f \circ h_0^{-1}$. Then (5.4) holds for $j = 0$. Moreover $h_0^{-1} h_1 = \pi = \pi_f = (h_0^f)^{-1} h_1^f$ implies

$$h_1^f \circ h_1^{-1} = h_0^f \pi_f h_1^{-1} = h_0^f \pi h_1^{-1} = h_0^f h_0^{-1} h_1 h_1^{-1} = \sigma, \tag{5.5}$$

which proves the lemma. □

We henceforth relabel the equilibria in the Sturm attractor $\mathcal{A}_f$ of the Sturm permutation $\pi_f = \pi = h_0^{-1} h_1$ such that the ZS-paths h_0, h_1 in G_2 also coincide with the boundary permutations h_0^f, h_1^f. With this labeling we can provide the final ingredient to the proof of Theorems 1.1 and 1.2.

Lemma 5.3. *The identity map between the vertices $v_1, \dots, v_N$ of the given filled graph G_2 and the equilibria of the connection graph $\mathcal{C}_f$ for the Sturm permutation π_f provides a graph isomorphism.*

Proof. In the proof of Lemma 5.1 we have seen how the Morse type of vertex v_k in G_2 coincides with the Morse index $i_k = i(v_k)$ of the equilibrium v_k in $\mathcal{C}_f$. This justifies the terminology Morse type, Morse sink, etc., which we have introduced. It also settles the direction of heteroclinic orbits in $\mathcal{C}_f$, from higher to lower Morse index, once it has been shown that the graphs G_2 and $\mathcal{C}_f$ are indeed isomorphic in the sense explained below Theorem 1.1. The given graph G_2 is the filled graph of its 1-skeleton G, by definition. The connection graph $\mathcal{C}_f$, likewise, is the filled graph of its 1-skeleton $\mathcal{C}_f^1$, by Theorem 4.1. It only remains to show, therefore, that both 1-skeletons possess the same edges and faces. Since edges connect vertices of adjacent Morse type, alias Morse index, in $\{0, 1, 2\}$ it suffices to show that each Morse saddle possesses the same edges attached to it, when considered in G_2 and $\mathcal{C}_f$. We first consider the nontrivial case of edges to saddles v which come from a source w. This will also settle the case of edges from those saddles to sinks. The remaining case of edges from saddles v, which are not adjacent to any sources, to sinks will then be trivial.

Let therefore w denote any (Morse) source, $i(w) = 2$, in G_2 and $\mathcal{C}_f$. The face F of w in $\mathcal{C}_f$, the corona ∂F, and the heteroclinic orbits in this set have been described in Section 4; see Theorem 4.1 and Fig. 7. For our analysis of this case, we will switch to the notation $v_1, \dots, v_{2n}$ for vertices in the corona, and $w = v_{2n+1}$ for the source, as employed there, both for G_2 and $\mathcal{C}_f$.

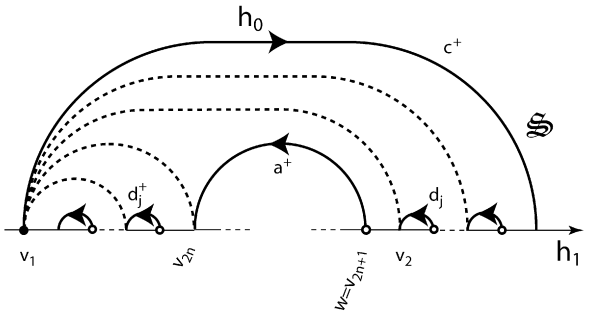

Fig. 10. Hamiltonian paths h_0 and h_1. Dashed arcs indicate saddle-sink heteroclinic orbits which separate Morse sources of adjacent faces.

The graphs G_2 and $\mathcal{C}_f$ are the filled graphs of G and $\mathcal{C}_f^1$, respectively. To show that G_2 is isomorphic to $\mathcal{C}_f$ in the closure of the w-face F, it is therefore sufficient to show that the (undirected) cycle ∂F in $\mathcal{C}_f$ is a cycle, likewise, in G without interior points in G. Consider the shooting map $\mathcal{S} = h_0$ and the horizontal path h_1 associated to the vertices in ∂F, as in Fig. 7. We recall that these are also paths in G_2 due to the straightening homeomorphism H in the proof of Lemma 5.1. Suppose we can show that G_2 possesses (dashed) pairs of edges

$$v_2v_1,\ v_{2n}v_1 \quad \text{and} \quad v_{2m}v_{2m+1},\ v_{2m+2}v_{2m+1} \tag{5.6}$$

located below c^+ but above all d_j^+, and above c^- but below all d_j^-, respectively. See Figs. 7 and 10. Then these edges will patch together with the h_0 shooting arcs $b_1, \ldots, b_{m-1}$, $b_{m+1}, \ldots, b_{n-1}$ and the attached horizontal h_1 segments $v_3v_4, \ldots, v_{2m-1}v_{2m}$, $v_{2m+3}v_{2m+4}, \ldots$, $v_{2n-1}v_{2n}$ to form an undirected cycle in G which is isomorphic to ∂F. Since $w \notin G$ is the only vertex of G_2 inside this cycle, ∂F is also isomorphic to a face boundary in G, as was claimed.

To settle the question of isomorphic saddle connections in the closure of faces F it therefore remains to establish the edges (5.6) of $\mathcal{C}_f$ to also be present in G_2. Substituting $v \mapsto -v$, as usual, we only need to address the pair $v_2v_1, v_{2n}v_1$. The analysis of Section 4 on orientations, shooting arcs, and Morse types alias Morse indices readily applies in G_2. The heteroclinic orbits $v_2 \rightsquigarrow v_1$, $v_{2n} \rightsquigarrow v_1$ of Theorem 4.1 alone have become meaningless in G_2 and must be replaced by a different argument.

The geometric situation above the horizontal h_1-axis is indicated in Fig. 10. The shooting arc c^+ emanates to the right, from the sink v_1. Below c^+ is the left running arc a^+ from source $w = v_{2n+1}$ to saddle v_{2n}. To the left of a^+, below c^+, similar left running source-saddle arcs d_j^+ may exists. Analogous arcs d_j may also exist to the right of a^+ below c^+. In absence of d_j, the arc c^+ of the shooting path h_0 terminates at v_2 and provides an edge v_2v_1 in G_2, directly. Analogously, the horizontal path h_1 provides the edge $v_{2n}v_1$ in absence of d_j^+.

In the general case consider the (undirected) cycle Γ in G_2 defined by the arcs a^+, c^+, d_j^+, d_j of h_0 and their connecting horizontal pieces of h_1. In G_2 the sources of the arcs a^+, d_j^+, d_j must then be separated from each other by saddle-sink edges, which emanate from each saddle in the arcs d_j, d_j^+, except d_1^+, into the interior of the cycle Γ. This follows because G_2 is the filled graph of its 1-skeleton G, and thus possesses only one single source in each face of G. The face separating saddle-sink edges are indicated by dashed arcs in Fig. 10. The only available sink on the cycle Γ to terminate all separating saddle-sink edges is v_1. In particular, G_2 contains the

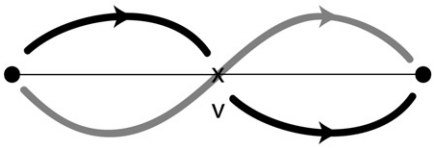

Fig. 11. A faceless saddle v.

saddle-sink edges v_2v_1 and $v_{2n}v_1$. This proves claim (5.6) and thus shows that any saddle on a face boundary in $\mathcal{C}_f$ possesses the same edges in $\mathcal{C}_f$ and in G_2.

The only remaining case concerns saddles v which are not on any face boundary of $\mathcal{C}_f^1$. See Fig. 11. Note that v cannot be on a face boundary of G either, by the above arguments, since faces of G and $\mathcal{C}_f^1$ already coincide.

The Hamiltonian paths h_0 and h_1 then must both pass through the faceless saddle v, in parallel. By definition (5.3) and Fig. 9 they disentangle as in Fig. 11. Therefore both edges of v in G_2 are also edges in $\mathcal{C}_f$. Moreover, these are all the edges of v in $\mathcal{C}_f$ because the one-dimensional unstable manifold $W^u(v) \setminus \{v\}$ consists of only two orbits, and the stable manifold $W^s(v) \setminus \{v\}$ does not intersect the Sturm attractor $\mathcal{A}_f$. This proves the lemma and, finally, completes the proof of Theorems 1.1 and 1.2. □

6. Bifurcation aspects

We conclude the paper with a discussion of parameter dependent behavior of global Sturm attractors $\mathcal{A}_{f_\lambda}$ associated to nonlinearities $f_\lambda = f(\lambda; x, u, u_x)$ in (1.1). See [13] for a general background on bifurcation theory. For simplicity of presentation we consider scalar real parameters λ, which can also be viewed as homotopies of the nonlinearities. Also for simplicity we stay with the case of Neumann boundary conditions (1.2); see the very analogous discussion of other separated boundary conditions in [17]. The somewhat different case $x \in S^1$ of periodic boundary conditions admits time periodic solutions, e.g., rotating waves, and has been addressed to some extent in [3,19,25,38,39].

Below we first discuss hyperbolicity of equilibria and pitchfork bifurcations, as manifested in the corresponding homotopies of the shooting curves $\mathcal{S}_\lambda$. As a first example we address the Chafee–Infante problem $f_\lambda = \lambda u(1-u^2)$ which historically was the first paradigm towards our investigations of general Sturm attractors. With this motivation in mind we discuss pitchforkable and non-pitchforkable Sturm attractors, including the simplest non-pitchforkable Sturm attractor as a second example. Generic one-parameter families f_λ feature only saddle-node bifurcations. As a third example we therefore review the pitchforkable n-gon attractors $\mathcal{A}_{n,m}$ of Section 3 and their genesis by saddle-node bifurcations. We then sketch an alternative approach to our results, suggested by Wolfrum [51], which proceeds recursively by removing faces from the boundary of the planar Sturm attractor. We conclude with an open question concerning the connected components of the set of dissipative nonlinearities f with associated hyperbolic Sturm attractors $\mathcal{A}_f$.

The k-dimensional Chafee–Infante attractor $\mathcal{A}^{\mathrm{CI}}(k)$ arises as $\mathcal{A}^{\mathrm{CI}}(k) = \mathcal{A}_{f_\lambda}$ for $f_\lambda = \lambda u(1-u^2)$ and $((k-1)\pi)^2 < \lambda < (k\pi)^2$, under Neumann boundary conditions (1.2). Note the planar case $\mathcal{A}^{\mathrm{CI}}(2) = \mathcal{A}_{2,1}$ of the 2-gon as illustrated in Figs. 2 and 5. Pitchfork bifurcations of the trivial solution $u \equiv 0$ at $\lambda = (k\pi)^2$ for $k = 1, 2, 3, \ldots$ are the only bifurcations of equilibria. See [11] for a detailed analysis of the bifurcation diagram including the Morse indices of equilibria. Following partial results in [14], the structure of the Chafee–Infante connection graph

$\mathcal{C}^{\mathrm{CI}}(k)$ has been clarified by Henry [34]. His analysis was based on the Sturm nodal property and the resulting transversality properties of stable, unstable, and center manifolds. See also [32]. In terms of Sturm permutations, which had not been introduced at that time, the Chafee–Infante attractors $\mathcal{A}^{\mathrm{CI}}(k)$ consist of $N = 2k + 1$ equilibria and correspond to the Sturm permutation $\pi^{\mathrm{CI}}(k) = (1, 2k, 3, 2k - 2, \ldots) \in S_{2k+1}$. It has been observed in [22] that the Chafee–Infante attractor is the unique Sturm attractor with the minimal number of equilibria, for any given dimension k.

After the work of Henry [34] and Angenent [1], the global consequences of sub- and supercritical pitchfork bifurcations on the connection graphs of Sturm attractors had been understood, due to these transversality properties of Morse–Smale type [43]. The term *pitchforkable* had been introduced to describe all attractors which could be generated by a sequence of pitchfork bifurcations. Note how pitchfork bifurcations are indicated by adjacency triplets $\pi = (\ldots, j \pm 1, j, j \mp 1, \ldots)$ in the Sturm permutation. For example $j = k + 1$ in the Chafee–Infante case. In terms of *ZS*-Hamiltonian pairs h_0, h_1 and for the planar case, pitchforkability is indicated by both paths running in parallel, or antiparallel to each other, for at least three consecutive vertices in the (filled) connection graph.

However, it was soon realized that not all Sturm attractors are pitchforkable. See [44] for a planar example with 11 equilibria and Sturm permutation $\pi = (1\ 8\ 7\ 2\ 3\ 6\ 9\ 10\ 5\ 4\ 11)$. Recently this turned out to be the unique planar non-pitchforkable example with minimal number of equilibria; see the self-dual case $11.3^2 - 3$ in [24].

Due to this example the pitchfork bifurcation, once so promising in the understanding of the Chafee–Infante problem, proved insufficient to investigate all Sturm attractors. The generic equilibrium bifurcation in one-parameter families f_λ is the saddle-node bifurcation anyway: two equilibria of adjacent Morse index merge and disappear by cancellation as the bifurcation parameter λ increases or decreases through the bifurcation point. At bifurcation the shooting curve $\mathcal{S}_\lambda$ exhibits a quadratic tangency with the horizontal $v(1)$-axis. As λ is varied, the shooting curve sweeps through the axis at nonvanishing speed, thus producing the coalescing pair of hyperbolic equilibria at the intersection points. Indeed transversality at the intersection is equivalent to hyperbolicity of the equilibria.

It is not too difficult to extend our results on hyperbolic Sturm attractors to a situation where generic saddle-node bifurcations of equilibria occur. Unfolding each saddle-node equilibrium to a pair of hyperbolic equilibria, the limiting saddle-node simply inherits all their known heteroclinic connections to any other equilibria. Because the transversality results of [1,34] include the center parts of invariant manifolds, all heteroclinic connections of saddle-node equilibria can be detected by this procedure.

Saddle-node bifurcations were the crucial tool in our combinatorial characterization of Sturm permutations as dissipative Morse meanders in [21]. In fact we proved that any dissipative Morse meander is indeed a Sturm permutation, inductively, by *retraction of noses*. We illustrate this process via the example of the Sturm permutation $\pi_{n,m}$ of the n-gon attractor $\mathcal{A}_{n,m}$ and its shooting curve; see Fig. 6. We first remove the $n - m - 1$ "noses" defined by the $n - m - 1$ arcs $(2, 3), \ldots, (2(n - m) - 2, 2(n - m) - 1)$ below the horizontal axis, via saddle-node bifurcations. Here arcs are labeled by the numbers of their start and end points, as indicated below the horizontal axis. Similarly we may remove the $m - 1$ arcs $(2(n - m) + 2, 2(n - m) + 3), \ldots, (2n - 2, 2n - 1)$. This produces the pitchforkable planar Chafee–Infante attractor $\mathcal{A}^{\mathrm{CI}}(2)$. Alternatively we could have inspected the Sturm permutations $\pi_{n,m}$ in (3.5) to see that all these permutations are indeed pitchforkable.

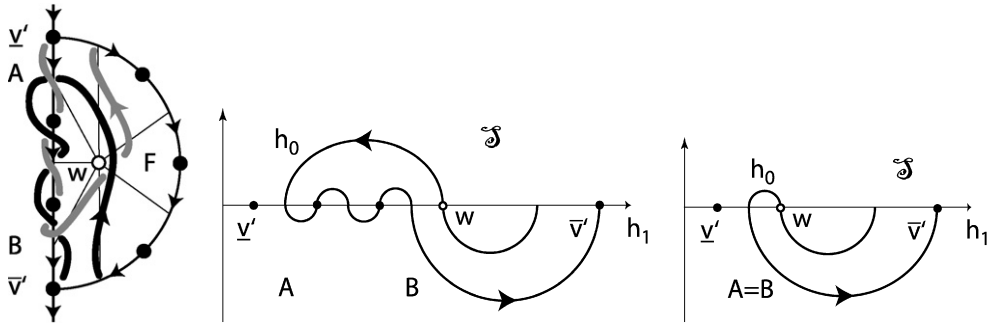

Fig. 12. Removable face F on left boundary of connection graph, (a), with corresponding shooting curve, (b), and simplified shooting curve, (c), before final nose retraction to remove F. Black: Z-Hamiltonian path h_0. Gray: S-Hamiltonian path h_1.

We are now prepared to sketch an alternative a posteriori approach to our present results, suggested by Wolfrum [51]. The idea is to reduce planar Sturm attractors, recursively, by removing faces from their boundary. Omitting almost all necessary detail, this procedure lends itself to an inductive proof of Theorems 1.1 and 1.2: just chase orientations, *ZS*-Hamiltonian pairs, and connections graphs through the successive attachment of suitably oriented faces to the existing boundary.

To remove a boundary face F by a nose retracting homotopy in the spirit of [21] we proceed as follows. We call a face F of the 1-skeleton $G = \mathcal{C}^1$ a *boundary face* if F shares at least one edge with the boundary ∂G. We consider G endowed with an orientation as in Theorem 1.1. Faces inherit this orientation. We call the oriented boundary face F *removable* if the di-source $\underline{v}'$ and the di-sink $\bar{v}'$ of the boundary of F itself also lie on the boundary ∂G. This may not be the case for all faces, but we claim that at least one such face exists along each of the two (left and right) boundary paths from $\underline{v}$ to $\bar{v}$ in ∂G. Indeed this is an easy consequence of the absence of di-critical vertices other than $\underline{v}$ and $\bar{v}$. See Fig. 12(a).

Calling the boundary face F removable is justified: we will remove F by a one-parameter homotopy f_λ of the nonlinearity. By the rules of Section 1 for *ZS*-Hamiltonian pairs (h_0, h_1) the paths h_0 and h_1 have to traverse the removable face F as indicated. Therefore the associated shooting curve looks as in Fig. 12(b). Eliminating the equilibria from A to B by a saddle-node cancellation, as above, we arrive at Fig. 12(c). The arrow in Fig. 12(c) indicates how to retract the remaining nose by a saddle-node cancellation of the Morse saddle $A = B$ against the Morse source w. It has been established in [21] that this retraction can indeed be realized by a suitable homotopy f_λ of nonlinearities. We refer to that paper for the delicate details of the precise realization of homotopies of shooting maps by one-parameter families $f_\lambda = f(\lambda; x, u, u_x)$. After retraction of the final nose in Fig. 12(c) the Morse source w has been removed, along with the Morse saddles A, B and all equilibria between them. This removes the boundary face F and justifies calling F removable.

Applying the removal procedure repeatedly, the original attractor $\mathcal{A}_{f_\lambda}$ can be reduced to a one-dimensional line. Any line can then trivially be reduced to a single equilibrium, either by a sequence of pitchforks, or by a sequence of generic saddle-nodes. Conversely we may build any planar Sturm attractor, from a line, by repeatedly attaching suitable n-gons to one of the two boundary paths from $\underline{v}$ to $\bar{v}$. The attached cells F must be oriented such that their local extrema $\underline{v}'$ and $\bar{v}'$ come to lie on the original boundary. By our above remarks, such a "swallow's nest" con-

struction will generate all planar Sturm attractors. It is therefore viable to recover Theorems 1.1 and 1.2, by induction over the number of faces, in a swallow's spirit.

We conclude with a question which has first been asked in [22]. Consider the space $\mathcal{F}$ of C^2 differentiable dissipative nonlinearities f in a suitable Whitney topology. On the set $\mathcal{F}_{\text{hyp}}$ of $f \in \mathcal{F}$ with only hyperbolic equilibria we obtain associated Sturm permutations π_f. Because hyperbolicity is equivalent to transversality of the shooting curve to the horizontal axis, the permutation π_f remains constant on each path connected component of $\mathcal{F}_{\text{hyp}}$. Do the levels of π characterize the connected components of $\mathcal{F}_{\text{hyp}}$? In other words, suppose $\pi_{f_0} = \pi_{f_1}$ coincide for some $f_0, f_1 \in \mathcal{F}_{\text{hyp}}$. Does there exist a homotopy path f_λ from f_0 to f_1 in $\mathcal{F}$?

A positive answer has been given in the class of finite-dimensional Jacobi systems, which admits a Sturm theory completely analogous to the above PDE case. See [22] and the references there for details. Even for the planar case considered in the present paper, however, and in our somewhat more restrictive PDE context the question remains open.

Acknowledgments

For bearing endless discussions with limitless enduring patience we are much indebted to Stefan Liebscher. We are also grateful to the Division of Applied Mathematics and the Lefschetz Center of Dynamical Systems at Brown University for their wonderful hospitality, and to Jörg Härterich for numerous helpful remarks. Beautifully expert typesetting was performed by Madeline Brewster.

This work was partially supported by the Deutsche Forschungsgemeinschaft.

References

[1] S. Angenent, The Morse–Smale property for a semi-linear parabolic equation, J. Differential Equations 62 (1986) 427–442.
[2] S. Angenent, The zero set of a solution of a parabolic equation, Crelle J. Reine Angew. Math. 390 (1988) 79–96.
[3] S. Angenent, B. Fiedler, The dynamics of rotating waves in scalar reaction diffusion equations, Trans. Amer. Math. Soc. 307 (1988) 545–568.
[4] V.I. Arnol'd, M.I. Vishik, et al., Some solved and unsolved problems in the theory of differential equations and mathematical physics, Russian Math. Surveys 44 (1989) 157–171.
[5] A.V. Babin, M.I. Vishik, Attractors of Evolution Equations, North-Holland, Amsterdam, 1992.
[6] L.W. Beineke, R.J. Wilson (Eds.), Graph Connections. Relationships between Graph Theory and Other Areas of Mathematics, Clarendon Press, Oxford, 1997.
[7] P. Brunovský, The attractor of the scalar reaction diffusion equation is a smooth graph, J. Dynam. Differential Equations 2 (1990) 293–323.
[8] P. Brunovský, B. Fiedler, Numbers of zeros on invariant manifolds in reaction–diffusion equations, Nonlinear Anal. TMA 10 (1986) 179–193.
[9] P. Brunovský, B. Fiedler, Connecting orbits in scalar reaction diffusion equations, Dynamics Reported 1 (1988) 57–89.
[10] P. Brunovský, B. Fiedler, Connecting orbits in scalar reaction diffusion equations II: The complete solution, J. Differential Equations 81 (1989) 106–135.
[11] N. Chafee, E.F. Infante, A bifurcation problem for a nonlinear partial differential equation of parabolic type, Appl. Analysis 4 (1974) 17–37.
[12] V.V. Chepyzhov, M.I. Vishik, Attractors for Equations of Mathematical Physics, Colloq. AMS, Providence, 2002.
[13] S.-N. Chow, J.K. Hale, Methods of Bifurcation Theory, Springer-Verlag, New York, 1982.
[14] C.C. Conley, J. Smoller, Algebraic and topological invariants for reaction–diffusion equations, in: Systems of Nonlinear Partial Differential Equations, Proc. NATO Adv. Study Inst., Oxford, UK, 1982, in: NATO ASI Ser. C, vol. 111, 1983, pp. 3–24.
[15] A. Eden, C. Foias, B. Nicolaenko, R. Temam, Exponential Attractors for Dissipative Evolution Equations, Wiley, Chichester, 1994.

[16] B. Fiedler, Global attractors of one-dimensional parabolic equations: Sixteen examples, Tatra Mt. Math. Publ. 4 (1994) 67–92.
[17] B. Fiedler, Do global attractors depend on boundary conditions? Doc. Math. J. DMV 1 (1996) 215–228.
[18] B. Fiedler (Ed.), Handbook of Dynamical Systems, vol. 2, Elsevier, Amsterdam, 2002.
[19] B. Fiedler, J. Mallet-Paret, The Poincaré–Bendixson theorem for scalar reaction diffusion equations, Arch. Ration. Mech. Anal. 107 (1989) 325–345.
[20] B. Fiedler, C. Rocha, Heteroclinic orbits of semilinear parabolic equations, J. Differential Equations 125 (1996) 239–281.
[21] B. Fiedler, C. Rocha, Realization of meander permutations by boundary value problems, J. Differential Equations 156 (1999) 282–308.
[22] B. Fiedler, C. Rocha, Orbit equivalence of global attractors of semilinear parabolic differential equations, Trans. Amer. Math. Soc. 352 (2000) 257–284.
[23] B. Fiedler, C. Rocha, Connectivity and design of planar global attractors of Sturm type. I: Orientations and Hamiltonian paths, Crelle J. Reine Angew. Math. (2007), in press.
[24] B. Fiedler, C. Rocha, Connectivity and design of planar global attractors of Sturm type. III: Small and Platonic examples, 2007, submitted for publication.
[25] B. Fiedler, C. Rocha, M. Wolfrum, Heteroclinic orbits between rotating waves of semilinear parabolic equations on the circle, J. Differential Equations 201 (2004) 99–138.
[26] B. Fiedler, A. Scheel, Spatio-temporal dynamics of reaction–diffusion patterns, in: M. Kirkilionis, et al. (Eds.), Trends in Nonlinear Analysis, Springer-Verlag, Berlin, 2003, pp. 23–152.
[27] H. de Fraysseix, P.O. de Mendez, P. Rosenstiehl, Bipolar orientations revisited, Discrete Appl. Math. 56 (1995) 157–179.
[28] G. Fusco, C. Rocha, A permutation related to the dynamics of a scalar parabolic PDE, J. Differential Equations 91 (1991) 75–94.
[29] V.A. Galaktionov, Geometric Sturmian Theory of Nonlinear Parabolic Equations and Applications, Chapman & Hall, Boca Raton, 2004.
[30] J.K. Hale, Asymptotic Behavior of Dissipative Systems, Math. Surveys Monogr., vol. 25, AMS Publ., Providence, 1988.
[31] J.K. Hale, L.T. Magalhães, W.M. Oliva, Dynamics in Infinite Dimensions, Springer-Verlag, New York, 2002.
[32] H. Hattori, K. Mischaikow, A dynamical system approach to a phase transition problem, J. Differential Equations 94 (1991) 340–378.
[33] D. Henry, Geometric Theory of Semilinear Parabolic Equations, Lecture Notes in Math., vol. 804, Springer-Verlag, New York, 1981.
[34] D. Henry, Some infinite dimensional Morse–Smale systems defined by parabolic differential equations, J. Differential Equations 59 (1985) 165–205.
[35] O.A. Ladyzhenskaya, Attractors for Semigroups and Evolution Equations, Cambridge Univ. Press, 1991.
[36] H. Matano, Convergence of solutions of one-dimensional semilinear parabolic equations, J. Math. Kyoto Univ. 18 (1978) 221–227.
[37] H. Matano, Nonincrease of the lap-number of a solution for a one-dimensional semi-linear parabolic equation, J. Fac. Sci. Univ. Tokyo Sect. IA 29 (1982) 401–441.
[38] H. Matano, Asymptotic behavior of solutions of semilinear heat equations on S^1, in: W.-M. Ni, L.A. Peletier, J. Serrin (Eds.), Nonlinear Diffusion Equations and Their Equilibrium States II, Springer-Verlag, New York, 1988, pp. 139–162.
[39] H. Matano, K.-I. Nakamura, The global attractor of semilinear parabolic equations on S^1, Discrete Contin. Dyn. Syst. 3 (1997) 1–24.
[40] J. Palis, W. de Melo, Geometric Theory of Dynamical Systems. An Introduction, Springer-Verlag, New York, 1982.
[41] A. Pazy, Semigroups of Linear Operators and Applications to Partial Differential Equations, Springer-Verlag, New York, 1983.
[42] G. Raugel, Global attractors, in: B. Fiedler (Ed.), Handbook of Dynamical Systems, vol. 2, Elsevier, Amsterdam, 2002, pp. 885–982.
[43] C. Rocha, Heteroclinic connections in parabolic equations, in: Advanced Topics in the Theory of Dynamical Systems, in: Notes Rep. Math. Sci. Eng., vol. 6, 1989, pp. 205–211.
[44] C. Rocha, Properties of the attractor of a scalar parabolic PDE, J. Dynam. Differential Equations 3 (1991) 575–591.
[45] G.R. Sell, Y. You, Dynamics of Evolutionary Equations, Springer-Verlag, New York, 2002.
[46] C. Sturm, Sur une classe d'équations à différences partielles, J. Math. Pures Appl. 1 (1836) 373–444.
[47] H. Tanabe, Equations of Evolution, Pitman, Boston, 1979.

[48] R. Temam, Infinite-Dimensional Dynamical Systems in Mechanics and Physics, Springer-Verlag, New York, 1988.
[49] M. Wolfrum, A sequence of order relations: Encoding heteroclinic connections in scalar parabolic PDE, J. Differential Equations 183 (2002) 56–78.
[50] M. Wolfrum, Geometry of heteroclinic cascades in scalar parabolic differential equations, J. Dynam. Differential Equations 14 (2002) 207–241.
[51] M. Wolfrum, personal communication, 2007.
[52] T.I. Zelenyak, Stabilization of solutions of boundary value problems for a second order parabolic equation with one space variable, Differential Equations 4 (1968) 17–22.